Joining by forming of composite sandwich panels

Tomás Rocha Mota Martins Contreiras

Thesis to obtain the Master of Science Degree in

Mechanical Engineering

Supervisors: Prof. Carlos Manuel Alves da Silva

Prof. Ivo Manuel Ferreira de Bragança

Examination Committee

Chairperson: Prof. Rui Manuel dos Santos Oliveira Baptista

Supervisor: Prof. Carlos Manuel Alves da Silva

Members of the Committee: Prof. Luís Manuel Mendonça Alves

Engº João Pedro da Fonseca Matos Pragana

February 2019

Acknowledgements

I want to express my deepest gratitude to this project and to whoever was involved in it.
My deepest appreciation goes to my academic advisors, Prof. Carlos Silva, Prof. Ivo Bragança and Engº João Pragana, for their availability and professionalism during the project development, for sharing their knowledge and experience and for giving me important suggestions and guidelines, allowing me to choose and work autonomously.
I want to thank Manufacturing & Process Technology department of Instituto Superior Técnico for the support and access to Laboratory facilities which made possible to carry out this thesis investigation. I also want to mention the Laboratory staff, Mr. Farinha and Diogo Silva for their help during the experimentation phase.
I want to thank Dr. Azeddine Chergui from ThyssenKrupp Steel Europe AG, Germany, for the support in the experimental work by providing the raw material in which the investigation was based.
Lastly, I want to express my sincere gratitude to my family, girlfriend and friends, for their support and affection.

Resumo

Esta dissertação assenta no estudo e implementação de três processos de ligação por deformação plástica para ligar duas chapas Litecor® compósito sandwich, perpendiculares entre si.

Os processos de ligação foram projetados com base na ligação do tipo mortise-tenon e diferem no número total de estágios de deformação plástica.

Este estudo contempla simulação numérica dos processos de ligação, recorrendo ao programa I-FORM, bem como ensaios experimentais para produzir as ligações entre chapas de compósito sandwich. Verificou-se uma boa correlação entre resultados obtidos por ambas as abordagens. As ligações foram testadas por meio de ensaios destrutivos para avaliar a sua resistência mecânica.

O processo de ligação com um estágio apresentou resultados satisfatórios apenas para uma gama restrita de parâmetros geométricos, o que limitou a sua resistência mecânica. O processo de ligação com dois estágios revelou ser o processo menos eficaz uma vez que originou ligações com as menores resistências mecânicas. Por fim, o processo inovador com três estágios permitiu obter ligações com a maior resistência mecânica atribuída a uma maior robustez da junta.

Os resultados mostram que as forças envolvidas nos processos de ligação para produzir ligações entre chapas compósitos sandwich são inferiores a 15 kN. São, por isto, processos de ligação eficientes e fáceis de implementar quando comparados com adesivos, soldadura e ligação por parafusos/ rebites.

Palavras-Chave

Materiais compósitos sandwich; Ligação por deformação plástica; Ligação de chapas compósito sandwich; Experimentação; Modelação por elementos finitos;

Abstract

This dissertation is based on the study and implementation of three joining by forming processes to join two Litecor® composite sandwich panels, perpendicular to one another other.
The joining processes were designed based on the mortise-tenon joint. They differ in the total number of forming stages.
The development run from finite element modelling, using the in-house finite element computer program I-FORM, to experiments in a laboratory tool setup. Good overall correlation between the simulation and the experiments is revealed. The joints were tested under destructive tensile testing.
The single-stage joining process presented good results only for a restricted range of the specimens tested, which limited the mechanical strength of the bonds. The two-stage joining process proved to be the least efficient process since it produced joints with the smallest mechanical strengths. Finally, the innovative three-stage joining process allowed to obtain joints with the greater mechanical resistance. In this case failure is found to take place by cracking of the flat-shaped head of the joint instead of by unbending back to its original shape.
The results show that the required forming forces to produce the new metal-polymer joints are below 15 kN, allowing them to be an effective and easy to implement alternative joining method to current solutions based on adhesive bonding, welding and mechanical fastening.

Keywords

Composite sandwich panels; Joining by forming; Joining of composite sandwich panels; Experiments; Finite element modelling;

Contents

List of figures

List of tables

Abbreviations

AHSS	Advanced high strength steel
Al	Aluminium
BEV	Battery electric vehicles
CAM	Computer-Aided manufacturing
CFRP	Carbon fibre reinforced plastics
CO_2	Carbon Dioxide
CTE	Coefficient of thermal expansion
DIN	German institute for standardization
FCEV	Fuel cell electric vehicle
FEM	Finite Element Method
FLC	Forming limit curve
FLD	Forming limit diagram
FSW	Friction stir welding
GFRP	Glass fibre reinforced plastics
GHG	Greenhouse gas
HEV	Hybrid electric vehicles
LBW	Laser beam welding
MPM	Metal-polymer-metal
MIT	Massachusetts institute of technology
NVH	Noise vibration and harshness
OEM	Original equipment manufacturer
PA	Polyamide
PC	Polycarbonate
PE	Polyethylene
PHEV	Plug-in hybrid electric vehicles
PP	Polypropylene
PU	Polyurethane
R&D	Research and development
RSW	Resistance spot welding
SBMF	Sheet-bulk metal forming
SPR	Self-pierce riveting
SPS	Steel-polymer-steel
UHSS	Ultra-high strength steel
VDSS	Vibration damping steel sheet

Units

m	Meters
cm	Centimeters
mm	Millimeters
µm	Micrometre
Kg	Kilogram
N	Newton
kN	Kilonewton
MPa	Megapascal
K	Degree Kelvin
◦C	Degree Celsius

Nomenclature

Symbols

Greek

Δ	Variation
ε	True Strain
σ	True Stress
φ_1	Larger logarithmic elongation
φ_2	Smaller logarithmic elongation
α	Thermal linear expansion coefficient
θ	V-punch included angle
β	Flange opening angle
ω	Angular velocity of the circular saw blade

Latin

A_0	Initial cross-sectional area of the stack compression specimen
A_i	Instant cross-sectional area of the stack compression specimen
D_0	Initial diameter of the stack compression test specimen
d	Punch displacement
F	Vertical load
F_i	Instant Force of the punch in stack compression test
h_0	Initial height of the stack compression test specimen
$\mathrm{h_i}$	Instant height of the stack compression specimen
i	Number of experimental test
j	Clearance between the tenon and the mortise
L	Litecor® panel length
l_h	Length of the head joint
l_t	Free-length of the tenon
T	Temperature
t	Thickness of the panel
t_c	Thickness of core material
t_s	Thickness of skin material
t_h	Thickness of the head joint
V_0	Initial volume of the stack compression specimen
V_i	Instant volume of the stack compression specimen
W	Litecor® panel width
w_h	Width of the head joint
w	Width of the mortise and tenon

1. Introduction and motivation

The automotive sector is undergoing rapid transformation much owed to a significant interest worldwide to minimize greenhouse gas (GHG) emissions. The upcoming emission regulations (Figure 1.1) are forcing automotive manufacturers to increase low-emission drive systems production, like hybrid electric vehicles (HEV) or plug-in hybrid electric vehicles (PHEV), and zero-emission drive systems production like battery electric vehicles (BEV) or fuel cell electric vehicle (FCEV).

The trend is clear and straightforward: to make all future vehicle generations lighter and therefore more fuel-efficient, capable to waste less resources whether it is fossil fuels or electric energy. Nevertheless, future vehicle generation must preserve all the safety, functionality and comfort requirements.

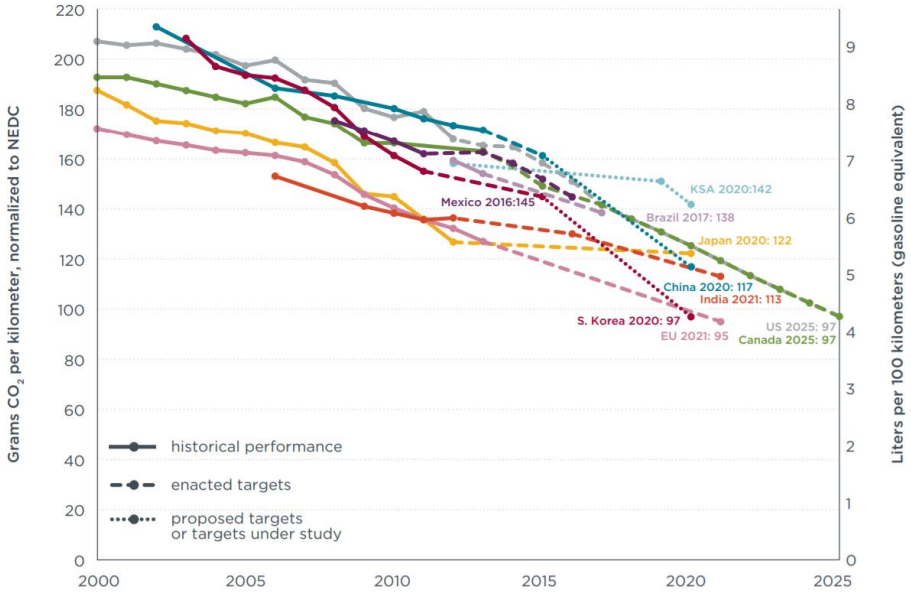

Figure 1.1 - Comparison of light-duty vehicle efficiency standards (passenger cars only, light-duty trucks excluded) [1]

For instance, new cars sold in Europe will have an emission limit of 95 grams of CO_2 per kilometre by 2021. Right now, leading companies are still 30 grams above this target [2].

Vehicle lightweighting is a concept used in the auto industry, it means to build vehicles that are lighter to achieve better fuel efficiency hence more environmentally friendly. It is mostly achieved through a combination of design optimization, downsizing and the use of lightweight materials. This concept is being pursued by automakers around the world as the main strategy to meet 2025 regulatory and market goals [1].

According to a MIT study [3], reduction in vehicle weight can significantly reduce fuel consumption and so the emissions. Every 10% of weight reduced from the average new car or light truck can cut fuel consumption by around 7%. For these reasons, new generations of automobiles look forward to containing a larger quantity and diversity of new advanced materials, lighter and thinner, in their components.

In what concerns car manufacturing one of the most relevant part for weight reduction efforts is the car body because it typically represents up to 40% of the total car weight [4]. Automakers are implementing

larger use of lighter materials on the vehicle body such as aluminium, magnesium, ultra-high strength steel (UHSS) and advanced high strength steel (AHSS), and polymer composite materials such as glass (GFRP) or carbon fibre reinforced plastics (CFRP) and others, Figure 1.2 [5]. A multi-material body design uses different material combinations within a same part or assembly for optimizing weight and performance.

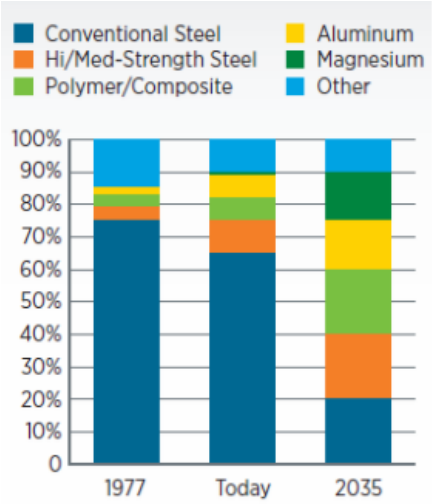

Figure 1.2 - Material usage and trend in automotive industry [5]

Due to the importance of this subject, there are some parties creating R&D projects on car body lightweight design such as automotive original equipment manufacturers (OEMs), material manufacturers/ suppliers (steel, aluminium and composite producers) and research organisations. One example of such projects is InCar®plus, a project created by Thyssenkrupp steel Europe which is one of the world's leading supplier of high-grade flat steel.

InCar®plus developed an innovative material product called Litecor®. It consists in a composite material classified as Metal/polymer/metal (MPM) sandwich material as it is composed of three layers: polymer core layered between two steel sheets, recalling the same idea of a sandwich, from which it gets the name of steel sandwich panel. Lightweight body design can be leveraged using such modern sandwich product for the outer panel combined with an optimized inner structure.

The layered structure that permits enhanced properties of MPM composites, creates challenges regarding manufacturing and processing (forming and joining).

Several researches focus on the forming behaviour of MPM materials [6-10] and only a few researches have been focused on the joining topic of multi-layer MPM systems.

To fully achieve the lightweight potential of sandwich composites, robust and cost-effective joining technologies, must be implemented to integrate these materials into assembly line-solutions. The implementation of new sandwich materials leads to the challenge of joining them together and attaching other vehicle parts to them [11]. Therefore, investigations on improving existent joining technologies or develop new and more suitable ones for various combinations of such high strength to weight materials are highly desired by the industry to make these materials more affordable and widespread.

Technical solutions capable of being used cost-effectively under volume production conditions have been developed in close cooperation with customers from the auto industry. Up until now, some proven joining technologies are available for integrating finished MPM parts. Due to the polymer core layer, cold

mechanical joining methods, like joining-by-forming or mechanical fastening in combination with adhesive bonding are preferable to thermal joining processes like welding processes. In welding the high heat input can lead to thermal deterioration of the polymer layer.
OEMs are looking for weight reduction opportunities no matter how small they are. This trend is leading to alternative lightweight joining technologies which do not utilize any consumables or external component and hence do not add weight.

1.1. Statement of purpose

Under the circumstances mentioned above, the main purpose of this thesis, in broad terms, is to present an alternative lightweight joining solution to assemble an advanced lightweight material, the metal-polymer composite sandwich, aiming to fully achieve its low weight potential.
This thesis investigates the feasibility and workability of three proposed joining by forming processes to join longitudinally in position two steel-polymer-steel (SPS) sandwich panels, perpendicular to one another.
To fulfil the thesis' purpose, the following tasks were performed:

- Numerical modelling using FEM to simulate and support the joining processes under investigation.
- Experimental testing to produce joints between two SPS sandwich panels in a T-joint configuration, perpendicular to one another.
- Destructive testing to evaluate the joint strength.

The research conducted allows the production of lightweight joints giving a perception of the workability window as a function of the major joining process parameters and demonstrates the feasibility of the new proposed joining by forming processes.
The result of the research will provide alternative joining by forming solutions for composite sandwich panels, which aims to clarify and recommend the joining processes nomenclature, joint design strategy, metrics and testing. It also aims to accelerate knowledge transfer, trigger meaningful discussions and to identify opportunities for further research collaboration among design and process engineers regarding the joining topic of MPM sandwich composites.
The contribution to knowledge of this thesis is the fundamental research into the use of new joining by forming methods to join MPM sandwich panels, concretely SPS sandwich panels, like Litecor®.

1.2. Thesis outline

This thesis is organized in six chapters. This introduction forms **Chapter 1** which discusses the background of the topic being studied according to current facts highlighting existent gaps and presenting a potential solution as the purpose of the research.

Chapter 2 is the state of the art, it details the relevant literature supporting the thesis work, namely the classification of metal-polymer composite sandwich materials and the main characteristics of the specific material being joined, Litecor®. Furthermore, the joining challenge of this type of materials is discussed and all the current available joining technologies for metal-polymer sandwich panels are presented. The

final subchapter gives an introduction to the type of joint developed in this thesis, mentioning some research works already developed in the subject.

In **Chapter 3**, the particular joining by forming processes investigated in this research are described, highlighting the step sequence, the geometrical properties, die usage and intended flow of material in each joining process. Also, the numerical modelling carried out to support the investigation is presented.

Chapter 4 presents the methodology by which the experiments were performed. This includes the identification of all equipment used, the metallography preparation of the specimens in which the tests were performed, and a description of each test procedure.

Chapter 5 details the results based on the joining processes tested to join two Litecor® panels perpendicular to one another and discusses the feasibility and workability of the joining processes based on the main process parameters.

Lastly, in **Chapter 6** a summation of the work done is given by referring the final remarks including the conclusion as well as the further work required to consolidate and extends the investigation developed.

2. State of the art

This chapter will cover the relevant literature survey regarding this thesis study. It is divided in three subchapters. The **first subchapter** presents the MPM sandwich materials, including their structure, their manufacturing process and their types. Also, this subchapter, gives an introduction to Litecor®, the composite sandwich panel under investigation, highlighting Litecor®'s mechanical properties, failure mode and potential application. In **subchapter two** the joining challenge of sandwich composite panels is discussed and their current available joining technologies are presented.
The knowledge of all the previous topics are relevant as they support the thesis goal.

2.1. Composite materials

Composite materials consist in the combination of two materials of different natures in one component aiming to retain the desired properties and eliminate the undesired ones of the starting materials. Composite materials are commonly used in the field of lightweight design and can be categorized according to their structure [12] as listed in Figure 2.1.
An innovative type of composite materials, the composite structural sandwich panels, or in short composite sandwich panels are raising interests in many applications in automotive, aerospace, marine and also construction [13] sectors because they gather numerous advantages such as economical weight saving, high rigidity combined with higher strength to weight ratio, high bending stiffness, high load carrying capacity, increased fatigue life, increased fracture toughness, improved thermal and acoustical insulation (vibration damping). They also need to be durable under severe service conditions, joinable and formable (deep drawing and bending).

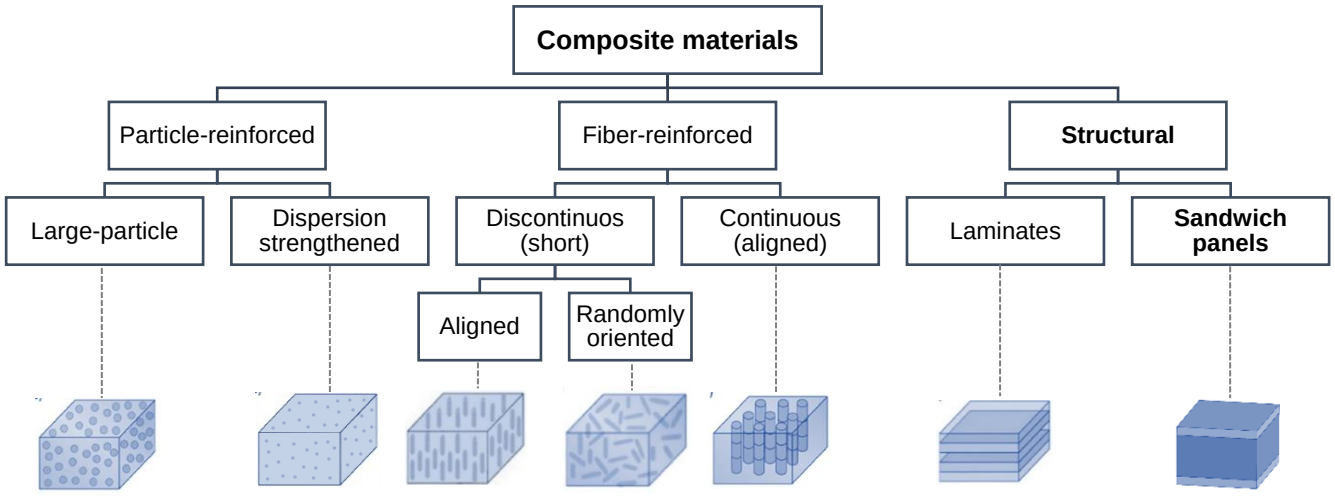

Figure 2.1 - Types of composite materials [12]

2.1.1. Structure of MPM composite sandwich panels

Metal-polymer-metal sandwich panels are composed by three discrete layers bonded together. The stiff skin material (metal layers) are on the outer surfaces separated by a polymer core as illustrated in Figure 2.2. Due to the low density of polymers (approx. 1/8 of steel) they are a good option for light-weighting being capable of increasing the bending stiffness of the composite without adding weight, keeping a low mass per unit area. According to material thickness, sandwich materials are designated in the following manner: skin layer thickness (t_s)/ core layer thickness (t_c)/ skin layer thickness (t_s), example (0.20/0.40/0.20).

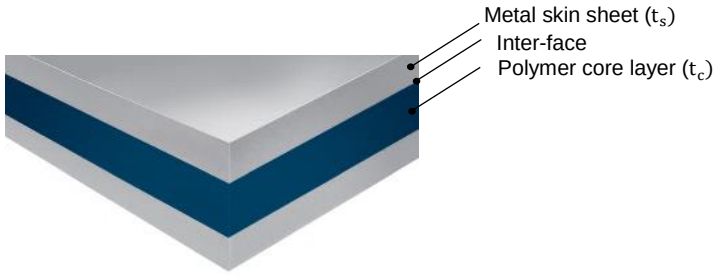

Figure 2.2 - Basic structure of an MPM sandwich panel

The basic structure of MPM sandwich panel combines the following three elements:

1. Two skin metal layers, which are relatively thin and possess high strength and good corrosion resistance. This layer will carry the loads and absorb most of the forming energy.

2. The inter-face between the skin metal layers and the core layer, which should offer a good adhesive strength, be durable, transmit the loads uniformly from the skin to the core to avoid forming defects, such as delamination and wrinkling.

3. Enclosed polymer core layer, which purpose is to act as a low-density filler with sufficient stiffness in a direction normal to skin layers capable to stabilize them under loading, to maintain a fixed distance between them and to transmit shear stresses through the layers [14]. It also should be durable against the processing and service conditions.

2.1.2. Production process of MPM composite sandwich panels

The most efficient technique used to manufacture MPM composites is Roll bonding. The Roll bonding steps are:

1. Pre-treating: the metal surfaces that will adhere with the polymer core are degreased with ethanol and then sanding to remove any contamination from the surface.

2. Bonding: the three components of the sandwich are bonded by two adhesion types. Indirect adhesion when a glue agent like polyurethane (PU) adhesive is used to increase or ensure the adhesion between polymer and metal layers and direct adhesion happens when the polymer itself behaves like an adhesive ensuring good bonding strengths [15].

3. Rolling the sandwich through a pair of flat rollers with a certain pressure and rolling speed, so that the deformation will ensure proper bonding.

When heat is involved in the process the technique is called Warm Roll Bonding (WRB) [16]. With this method the surfaces are heated up before the rolling process to increase the ductility and the strength of the bond. The process is shown in Figure 2.7. This type of manufacturing technique allows continuous production and cost reduction.

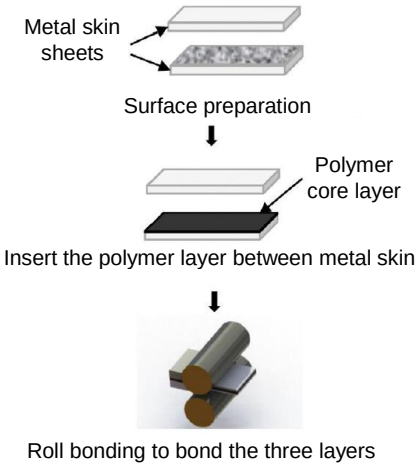

Figure 2.3 – Roll bonding process – schematic representation [15]

2.1.3. Different types of MPM composite panels

MPM composites can be categorized according to the type of core layer and intended function as shown in Figure 2.4 [17], [18]:

- The viscoelastic core type is used to produce vibration-damping sandwich panels. A thin viscoelastic adhesive represents less than 20% of the total thickness and bonds the two metal skins. These types of MPM composites are generally intended for noise (sound damping) and vibration reduction.
- The thermoplastic core type forms the lightweight sandwich panels which are composed of a thick core, 40 to 60% of the total thickness, bonded between the two metal skins. Lightweight sandwich panels are designed for their weight savings and high stiffness properties.

Both core types in combination with the metal skin layers offer high forming capabilities.
The layered structure of MPM composite panels may be symmetric or asymmetric. The asymmetry is introduced either by varying layer thicknesses or metal type/grade.

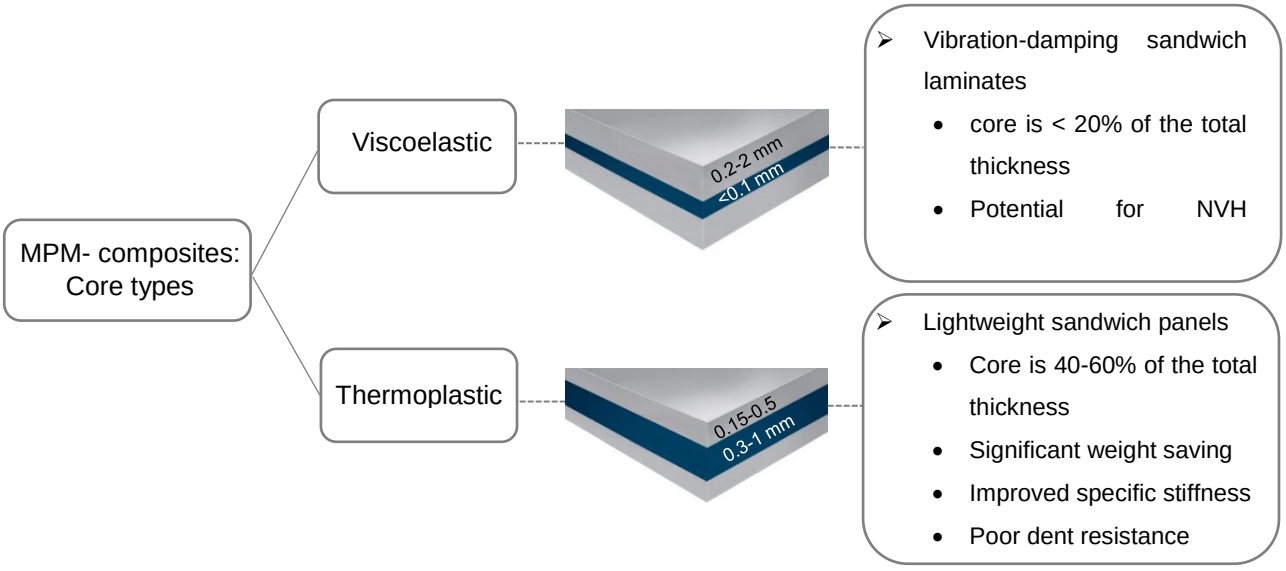

Figure 2.4 - Classification of MPM sandwich materials according to the core type [17,18]

The most common metals used in MPM composites are steel and aluminium. Depending on the application one can be preferable to the other based in three factors: cost, density and strength.

The main commercial MPM sandwich panels developed so far are listed in Table 2.1.

Table 2.1 - Main commercial MPM sandwich composites

Trade name	**Skin sheet**	**Core layer**	
Alucobond® PE	Al	PE	[19]
Bondal®	Steel	Viscoelastic adhesive	[20]
Hylite®	Al	PP	[21]
Litecor®	Steel	PE/PA	[22]
Steelite®	Steel	PP	[23]
Usilight®	Steel	PP, PP/PE	[24]

This thesis will focus its investigation on Litecor® composite sandwich panels.

2.1.4. Litecor®

Today, instead of having to choose between aluminium or carbon-fibre reinforced plastics (CFRP) previously the established lightweight materials for body parts, vehicle designers can now consider MPM composite sandwich materials as an option. One example is Litecor®, the trade name for a steel-polymer sandwich panel developed by ThyssenKrupp steel Europe, under the InCar®plus project [25]. Litecor® consists of an upper and lower cover sheet made from a high strength steel interstitial free, HX220, [26] which are attached to a polymer core layer, thermoplastic PA/PE compound, as shown in Figure 2.5 [27]. The two steel cover sheets in Litecor® are each electrolytically galvanized on both sides. The thickness dimensions of the steel cover sheets can vary from 0.20 mm to 0.50 mm and the

core layer thickness dimensions can vary from a minimum of 0.30 mm to a maximum of 1.00 mm. By adjusting layer thicknesses, the mechanical properties of the composite material can be configured to the specific application. Asymmetrical structures are also possible.

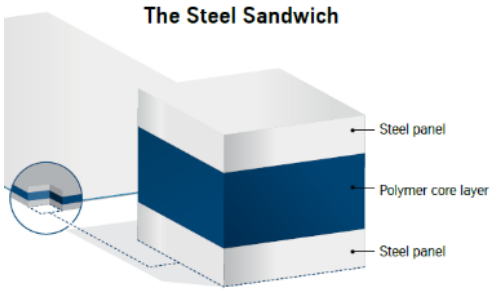

Figure 2.5 - Material structure of Litecor®: a three-layered composite [27]

Litecor® is produced by Warm Roll bonding, the manufacturing process in ThyssenKrupp steel Europe facilities is illustrated in Figure 2.6. The manufacturing process of Litecor® is a real challenge because the three layers must remain firmly bonded together under the effects of heat, severe forming, and ageing. Also producing steel sheets in such small thicknesses in the surface quality required by the industry is technically demanding. The exact production process is proprietary and confidential, but ThyssenKrupp can overcome the challenge by using the right combination of pressure, temperature and bonding mechanisms [27]

Figure 2.6 - Litecor® manufacturing process on site [27] [28]

The sandwich steel Litecor® is an alternative to aluminium with a goal of achieving at least 30% cost benefit compared to aluminium while only increasing weight by less than 10% [27]. Besides the attractive stiffness-to-weight ratio compared to conventional steel materials, Litecor® is also a natural acoustic, thermal and vibration damper due to the polymer core. This can indirectly reduce weight by making other damping materials redundant. The combination of steel and plastic allow Litecor® to possess the low cost of steel with the effectiveness of aluminium meaning that it is cheaper than aluminium and

significantly lighter than conventional steel sheet. Figure 2.7 shows a comparison between Litecor®, steel and aluminium.

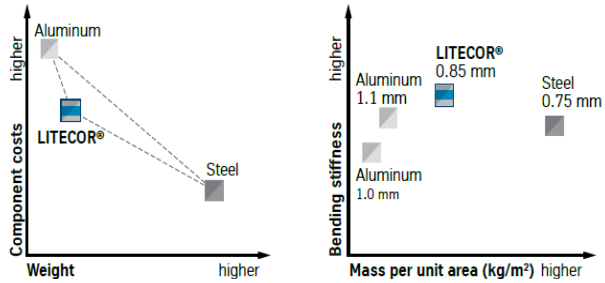

	Composition/ thickness	Mass per unit area	Bending stiffness
	mm	kg/m²	%
Aluminum	1.10	2.97	105
Aluminum	1.00	2.70	79
Reference: steel	0.75	5.80	100
LITECOR®	0.2 + 0.4 + 0.2 = 0.80	3.50	106
LITECOR®	0.2 + 0.4 + 0.25 = 0.85	3.90	129
LITECOR®	0.2 + 0.7 + 0.2 = 1.10	3.80	234

c)

Figure 2.7 - Comparison between Aluminium, Steel and Litecor®: a) Cost vs weight (qualitative); b) Bending stiffness vs Mass per unit area (qualitative); c) Bending stiffness (%) vs Mass per unit area (Kg/m^2) (quantitative) [29].

Parts made from Litecor® cause fewer CO_2 emissions in production than any other lightweight material and like all steel products, can be recycled endlessly with no loss of quality. So, Litecor® is a major step towards climate-friendly mobility.

As the first easy-to-process and low-cost sandwich composite material for use in modern car bodies, Litecor® facilitates weight and emission reductions that would be either impossible to achieve in large body parts with today's conventional lightweight steels or too expensive to achieve with alternative lightweight materials. Litecor® is entitled as the intelligent solution for cost-effective lightweight body design.

2.1.4.1. Mechanical properties

The mechanical properties relevant for the forming of the sandwich material are determined primarily by the steel face sheets. Their strength is much higher than that of the polymer core layer, so the forming limits are comparable with those of solid steel sheet. The forming limit curve (FLC) for Litecor® lies only slightly below that for a comparable solid steel sheet meaning that the processing of Litecor® and conventional steel panels in the press shop is almost identical – as it is typical for cold forming sheets, the form is changed through deep and stretch drawing in tools that may have been slightly modified.

Regarding thermal expansion, the properties of the steel face sheets dominate the behaviour of the sandwich material. The thermal linear expansion coefficient (CTE) of Litecor® is very similar to that of conventional steel sheet. This means that when a Litecor® part is installed in a steel environment, for example a sandwich roof in the body, no thermally induced stresses and strains are caused – a frequent problem with multi-material designs ($\alpha.\Delta T$ problem) [30]. Another thermal property relevant is the polymer decomposition temperature which happens for T>250ºC.

The composite adhesion of Litecor® is characterized by a peel strength of 250 N/cm. [31]

2.1.4.2. Failure modes

Sandwich composite materials may fail under the action of external loads. The main failure modes of MPM sandwich panels are:

- Failure of the adhesive bond (delamination). When a sandwich column is subjected to peel loading the adhesion between the face and the core may fail (Figure 2.8 a). [32]
- Face failure. When a sandwich column undergoes tensile loading, if the normal tensile stress in the face equals the yield strength for ductile skin materials and fracture strength for brittle face materials, the face or skin sheet may yield or fracture respectively, (Figure 2.8 b). [33]
- Euler macro buckling, core shear, micro-buckling and face sheet wrinkling failure modes occur when a sandwich column is subjected to end compression [34].
    - Euler macro-buckling, is a type of failure in which a column subjected to compression loading, becomes instable and pass instantaneously into a curved axis configuration, the column being said to have "bent". It is known simply as buckling, and it occurs because the compression level on the element reaches a certain value for which it is easier to "jump" to another configuration, even if much more deformed (curved). In forging operations buckling is a term used to describe the wavy condition of the workpiece caused by compressive stresses (Figure 2.8 c) [35].
    - Core shear is a failure mode occurring when the principal stresses in the core combine to exceed the yield criteria (Figure 2.8 d).
    - Micro-buckling of composite face sheets occurs when the axial stress within the compressive face sheet attains the face sheet micro-buckling strength, treated as an intrinsic material property (Figure 2.8 e).
    - Face wrinkling is a local instability of the faces involving short wavelength buckling of the face sheets, resisted by the underlying elastic core. It occurs when the normal stress in the compression face of the beam reaches the level of instability (Figure 2.8 f).

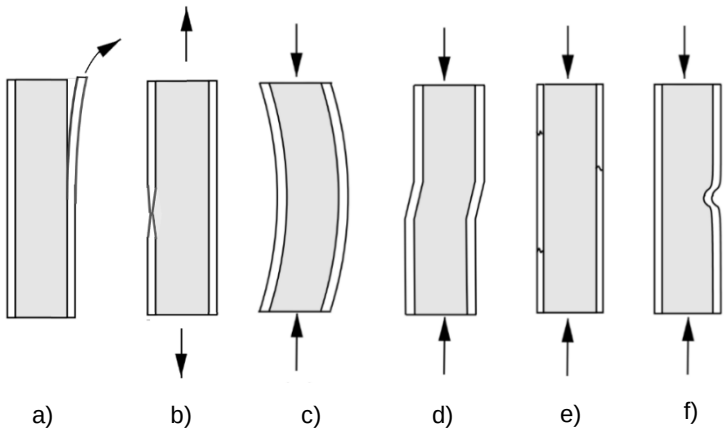

Figure 2.8 - Failure modes in sandwich columns according to three types of external loading: a)Delamination failure (peel loading); b) Face yielding failure (tensile loading); c) Euler macro-buckling (compressive loading); d) Core shear macro-buckling (compressive loading) e) face sheet micro-buckling (compressive loading) and f) face sheet wrinkling (compressive loading) [34].

2.1.4.3. Potential applications

In a study performed by Thyssenkrupp, the car body reveals potential for the application of 14 Litecor® parts divided in structural inner parts and outer panel components [36]. With the same performance, these are a total of 19.1 kg or around 20 % lighter than conventional components. Integrating Litecor® into the body-in-white is easy because it possesses the superior forming properties of conventional steel. Moreover, it is suitable for paint-shop.

Figure 2.9 illustrates the parts and Table 2.2 describes the corresponding layer structures. Figure 2.10 shows some real parts manufactured with Litecor® that were submitted to testing to ensure technical feasibility of part processing.

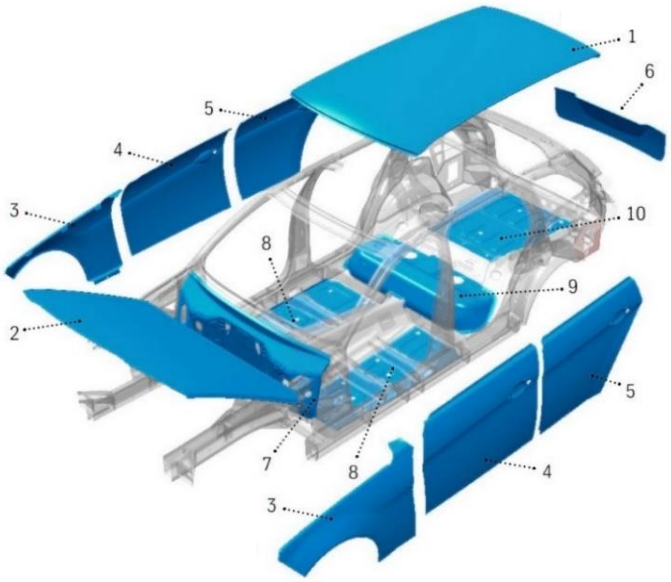

Figure 2.9 - Litecor® body parts potential application [36]

Table 2.2 - Overview of Litecor® body components and their layer structure [36]

	No.	Part	Composite structure (thickness of individual layers in mm)
Outer panel components	1	Roof outer panel	0.25/0.40/0.20
	2	Hood outer panel	0.25/0.40/0.20
	3	Fender front right/left	0.25/0.40/0.20
	4	Front door outer panel right/left	0.25/0.40/0.20
	5	Rear door outer panel right/left	0.25/0.40/0.20
	6	Tailgate outer panel	0.25/0.40/0.20
Structural inner	7	Firewall	0.25/0.40/0.25
	8	Main floor middle right/left	0.20/0.40/0.20
	9	Floor panel rear seat	0.25/0.40/0.25
	10	Floor rear	0.20/0.40/0.20

Litecor® parts are already used in the inner parts, development target is outer panel parts [37]. For instance, the application of Litecor® to produce a vehicle roof outer panel can save up to 7.29 kg corresponding to 38% weight reduction when comparing to the conventional steel roof and the weight reduction of a Litecor® rear door outer panel will be around 10% to the reference door [38].

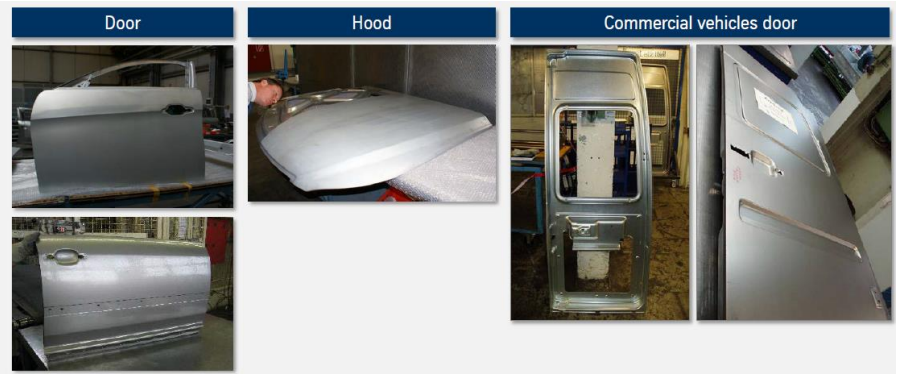

Figure 2.10 - Examples of successful production of parts from sandwich material Litecor® [39]

2.2. Joining of composite sandwich panels

The implementation of MPM sandwich panels implies the need of joining them together and attaching other parts to them. Joining becomes a challenge due to the layered structure of MPM sandwich panels, in particular because of the unavoidable properties of the polymeric core layer, which are:

1. Electrically insulator, which hinders the welding process.
2. Mechanically elastic and softness which leads to local dimension distortion and indentation under mechanical pressure.
3. Thermally instable at elevated processing and service temperature like welding and some coating processes.

A selection of joining technologies is already available to join metal-polymer sandwich composites and can be classified into four groups of joining processes: adhesive bonding, welding and two types of mechanical joining, mechanical fastening and joining by forming process (Figure 2.11).

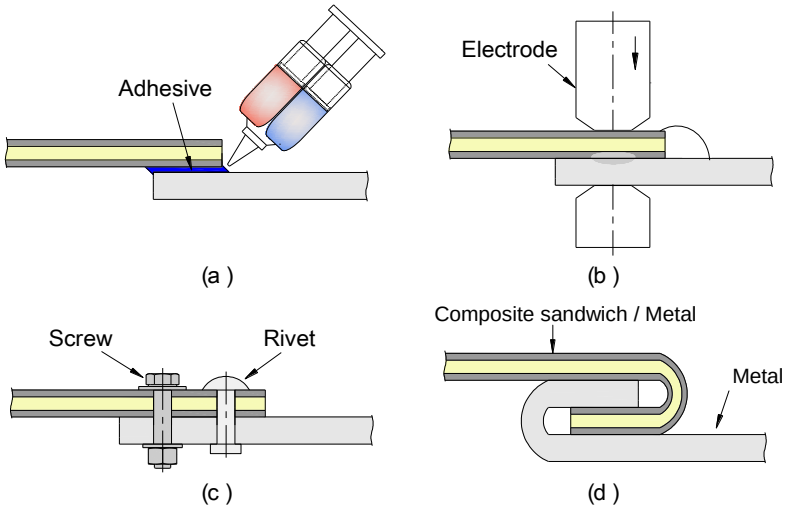

Figure 2.11 - Existing joining technologies to join metal-polymer composite sandwiches. a) Adhesive bonding; b) Welding-based technologies (e.g. spot welding); c) Mechanical fastening (e.g. screws and rivets); d) Joining by forming (e.g. hemming).

Due to the polymer core layer, cold mechanical joining methods, like mechanical fastening, in combination with adhesive bonding are suitable to join metal-polymer sandwich composites and preferable to thermal joining processes such as resistance spot welding (RSW) and laser beam welding (LBW). The high heat input of these two largely used welding processes can lead to thermal deterioration of the adhesion between plastic core and metal surface, to the point where the core is eventually destroyed. Friction stir welding (FSW) is a solid-state welding process that generates less heat so is capable to produce a joint keeping polymer layer's integrity.

Another alternative joining process is the joining-by-forming process, a subcategory of mechanical attachment technologies, which is based in complex forming operations involving plastic deformation of one or more joint component. For metal-polymer sandwich panels, the joining-by-forming technologies available is table-top hemming and roller hemming.

Although some of these joining technologies may not yet be ready for body shop applications where many production requirements must be met, further investment into research and development in these technologies may result in future high volume, industrial applications.

Next, it will be presented a detailed description of the current available joining technologies to join sandwich panels.

2.2.1. Adhesive bonding

Adhesive bonding joining process is a consolidated joining process in high technology industries such as aerospace, aeronautics and automotive industries. Adhesively bonded joints are increasing alternatives to mechanical joints in engineering applications and provide many advantages over conventional mechanical fasteners [40].

The materials being joined are called adherents, while the chemical agent is called the adhesive. This technology requires surface preparation, application and curing of the adhesives at room or elevated temperatures to produce permanent joints [41].

During the curing time, fixtures are used to lock and hold the metal-polymer sandwich composites in position for a certain bond line thickness and to ensure a uniform application of pressure. The process is schematically shown in Figure 2.12.

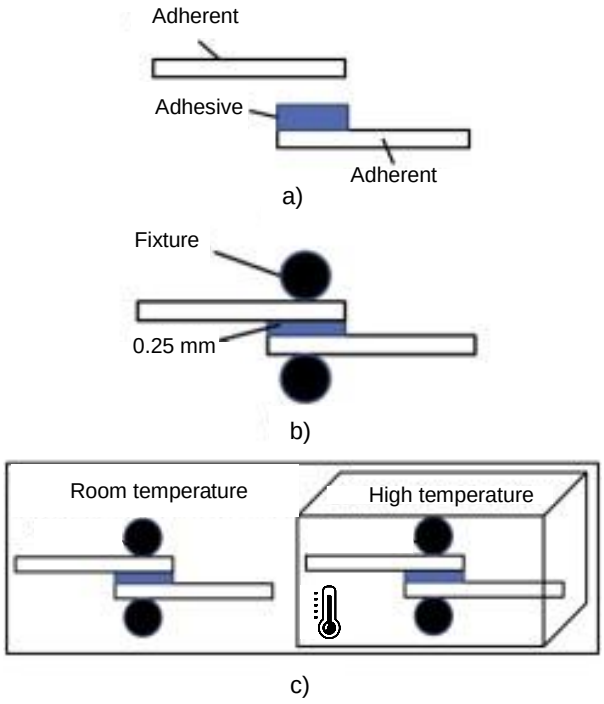

Figure 2.12 - – Schematic diagram of adhesive bonding process: a) Positioning and adhesive application, b) Pressure application, c) Curing [42].

Adhesive bonding can be applied to join MPM sandwich panels following the same process as for monolithic sheets, Figure 2.13 a), originating overlap joints. Adhesive bonding of sandwich panels can also be performed with the aid of overlaminates in joint configurations shown in Figure 2.13 b). The overlaminates will increase the adhesion area without the need of an overlap joint and will allow more joint designs.

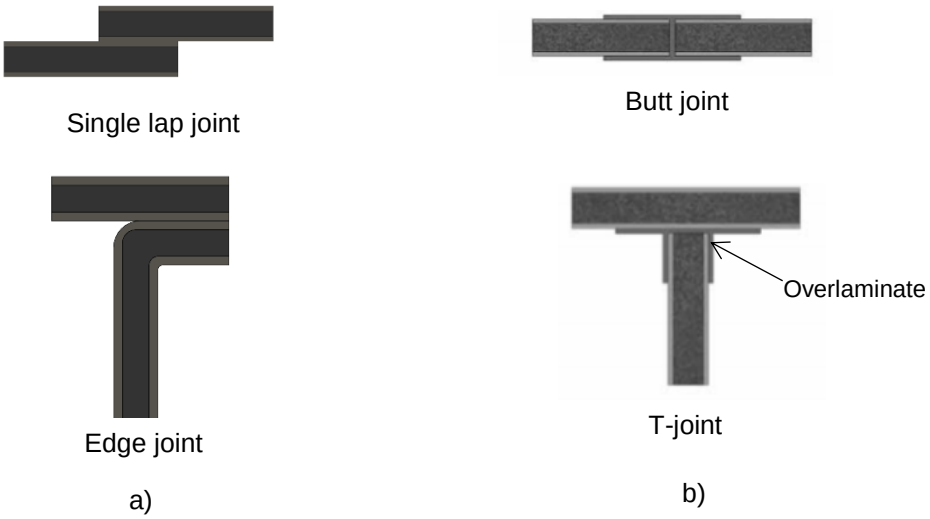

Figure 2.13 – Possible joint configurations for adhesive bonding sandwich panels: a) Overlap joints, b) joints with overlaminates [43].

The main advantages and disadvantages of adhesive bonding are summarized in Table 2.3.

Table 2.3 - Main advantages and disadvantages of adhesives for joining metal-polymer sandwich composites

Advantages	Disadvantages
• Minimal alteration of the chemical composition and microstructure of the adherents • Suitability to joining dissimilar materials and thicknesses • Uniform distribution of stress over the whole area of the joint • Sealing and insulating capability • Design flexibility and lower structural weight	• The need for surface preparation • Susceptibility to environmental degradation • Long curing times compromising the process productivity • Difficult inspection • Low level of automation • Severe problems may occur due to large differences of adherends thermal expansion • Overlap joints or the need to use overlaminates, leading to thick joints and weight gains

2.2.2. Welding

Welding is a thermal joining process in which metals are joined together through the formation of chemical bonds under the combined action of heat and pressure. The types of bonds formed across the joint are the same as the types of bonds found in the materials being joined.

MPM materials are conditionally suitable for thermal joining processes such as arc welding, resistance spot welding (RSW) and laser beam welding (LBW) because of their high energy inputs which may lead to thermal deterioration of the adhesion between plastic core and galvanized steel surface, to the point where the core is eventually destroyed.

Data from ThyssenKrupp report that gas metal arc welding like MIG/ MAG are not possible to join Litecor® [36]. Resistance spot welding (RSW) and Laser beam welding (LBW) can be used however they are subjected to some limitations.

- **Resistance spot welding**

ThyssenKrupp developed a new resistance spot welding process to qualify Litecor® for this process and for combined spot welding and adhesive bonding because both processes are used in body design assembly. Litecor® can be joined to the surrounding steel body components in the material pairings shown in Figure 2.14: single-lap joints (1 and 2) and double-lap joints (3 and 4).

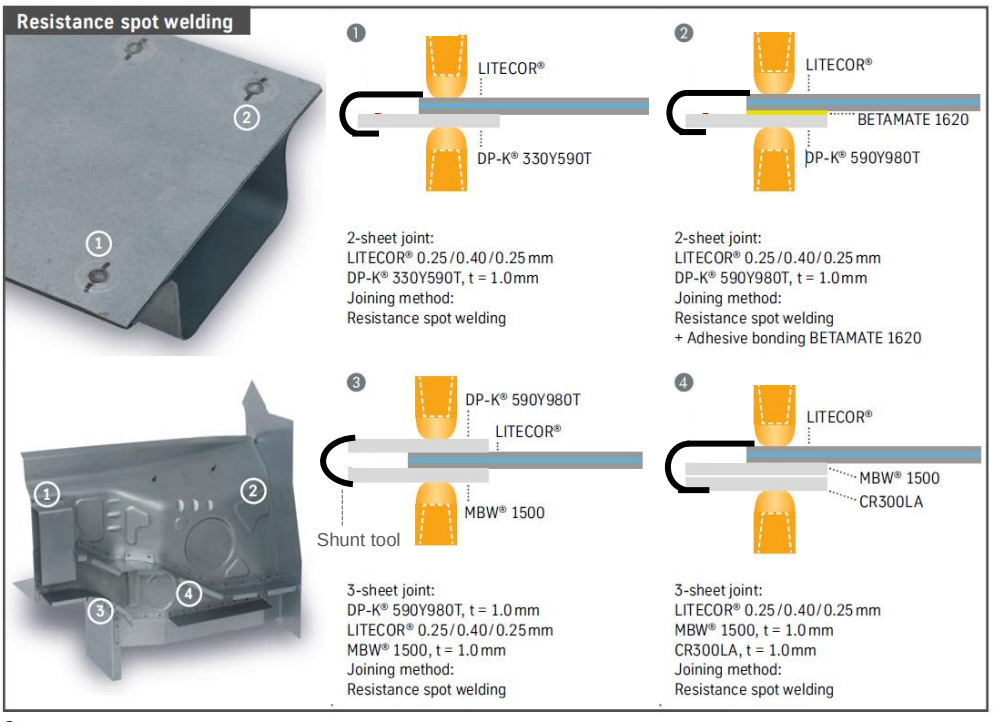

Figure 2.14 - Resistance spot welding of Litecor® with typical material pairings in body design [36]

The new resistance spot welding is slightly different from the standard process: a setup of a shunt connection is used to overcome the non-electrical conductivity issue by the polymer core. Figure 2.15 illustrates the idea for pairing number 3 of Figure 2.14. Litecor® panel layered between a dual-phase steel DP-K® 590Y980T [44] and a manganese-boron steel MBW® 1500 [45].

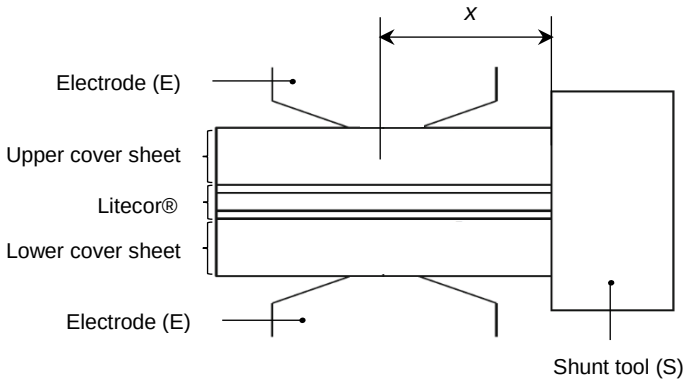

Figure 2.15 – RSW of sandwich composite panels: schematic representation [46]

This new resistance spot welding process is a two-step process requiring a dual-pulse power supply to perform a weld [46]: in the 1st step, the first pulse is responsible for making the current to pass through the metal layers and the shunt tool, as shown in Figure 2.16 a). The shunt tool needs to be close to the electrode/proposed welding area (dimension x in Figure 2.15). In the initial stage the total current equals the shunting current. This high current passing through the metal layers will heat them, the polymer core in the sandwich steel will be melted and the outer sheets will be pressed into contact under the weld force. Once all four metal sheets are in contact the 2nd step starts.

In the second pulse, current will flow directly in the welding area and the generated heat will melt the metal in this region forming the weld nugget, see Figure 2.16 b). For this reason, in the 2nd step the shunt tool must be far from the electrode, because if not some of the current will pass through the shunt tool and will lose part of the energy and affecting the welding quality. The total welding current at this stage is distributed between a welding current and a shunting current.

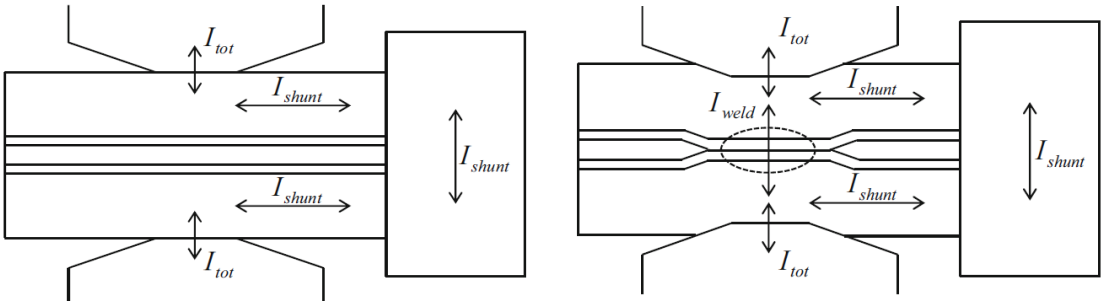

$$I_{tot} = I_{shunt} \quad (1)$$

$$I_{tot} = I_{weld} + I_{shunt} \quad (2)$$

a) b)

Figure 2.16 - The principle of RSW applied to composite sandwich panels: a) 1st step, b) 2nd step [46]

The risk of expulsion (severe eruption of molten material) is especially high in spot welding of sandwich steel due to very dynamic and unstable character of the process, associated with melting and squeezing out the polymer core at contact area in the first stage of the process [47]. A real experimental setup as well as a joint performed with Litecor® can be seen in Figure 2.17.

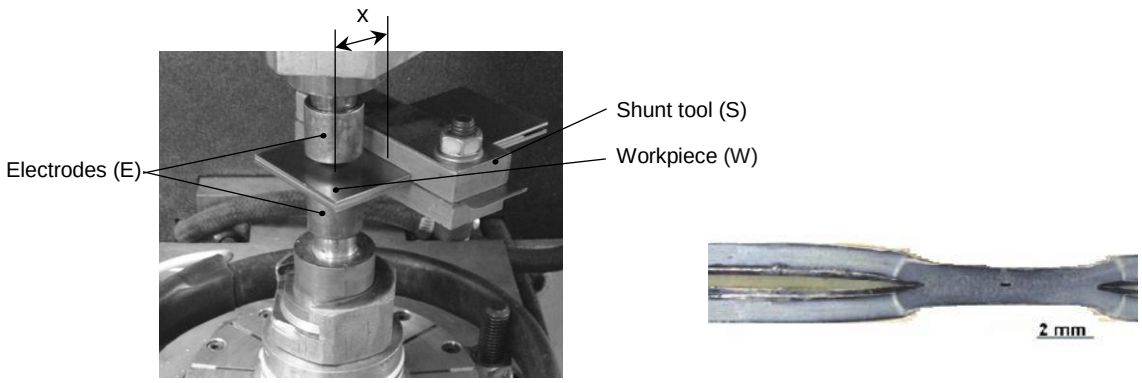

a) b)

Figure 2.17 – a) Experimental setup where the shunt tool (S) is mounted in on the stack-up of workpieces (W) in a distance d from the electrodes (E) [46]; b) Macrograph structure of a cross sectioned RSW joint [48]

The robustness of the process was confirmed once the requirements for joint quality and strength values were met, however it is still difficult to find the optimum values for RSW parameters: welding current, welding time, electrode force and its duration, electrode geometry. More research must be developed to optimize those parameters and qualify RSW process to be applied in sandwich composites for the auto industry.

The main advantages and disadvantages of RSW applied to steel sandwich sheets are summarized in Table 2.4.

Table 2.4 - Main advantages and disadvantages of RSW for joining steel-polymer sandwich composites.

Advantages	Disadvantages
• The process is comparatively low cost • Low skill labour requirements • There is no need for edge preparation	• Thermal degradation of the polymer • Unstable character of the process • Long joining times • Applicability restricted to overlap joints • High indentation of the electrodes leads to bad appearance of the welding area.

Steel-polymer sandwich panels have been rarely used in high volume applications, because RSW process requires long joining times. It is time consuming to carry out spot weld by providing a bypass circuit for every weld point.

To solve the non-conductivity issue of the polymer layer Akihiko Nishimoto and his team, developed the weldable VDSS sheet [49] which can be welded without the aid of a bypass circuit device by adding nickel particles to the resin layer to make the polymer a conductor. They also analysed many other particles additives with different sizes and they conclude nickel particles with size (44-74 μm) are the most optimum particles to make the VDSS spot weldable, however these solutions have a slight reduction of vibration damping performance [50].

- **Laser beam welding**

Laser beam welding (LBW) is a fusion welding process in which two metal pieces are joined together using a laser. It is a highly efficient technique applied in the production of automotive bodies, with comparatively small heat input which produces high quality welds.

The basic principle of LBW process as well as the identification of the main process players is illustrated in Figure 2.18. As the laser beam strikes the cavity between the two pieces to be joined, it melts the base metal from both parts and fuses them together.

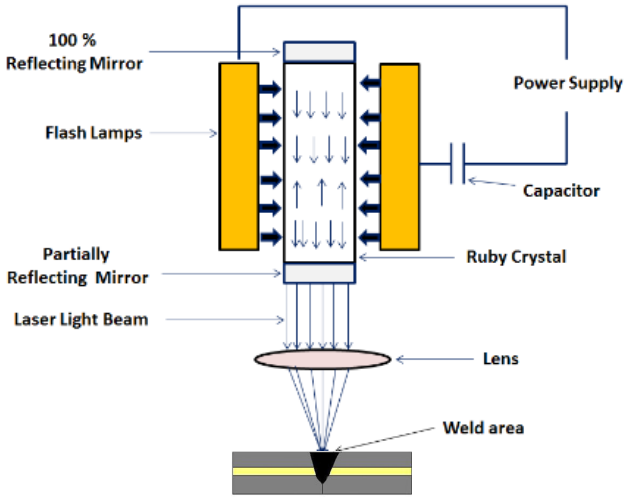

Figure 2.18 - Schematic illustration of remote laser welding process [51]

Published studies are available and prove that laser welding can be considered as an alternative joining process to join sandwich sheet composites in a butt joint configuration. Salonitis et al. [52] investigated theoretically two different approaches, one and two-sided laser welding, Figure 2.19 a) and b), to evaluate its impact on the polymer core layer. Laser welding should not damage the polymer core. The one-sided welding approach will result in the evaporation of some of the viscoelastic core [53]. Thus, controlling the amount of the core material to be sacrificed is significant. The main challenge of the two-sided approach is to control the depth of the welding through proper selection of process parameters, without having the temperature of the core raised above its melting temperature. A real example of a part joined by LBW under the two-sided approach is represented in Figure 2.19 c). The theoretical study has indicated that this is possible but still lacks in experimental verification. Future works need to focus on the selection of the process parameters' optimization to generate reliable process window maps.

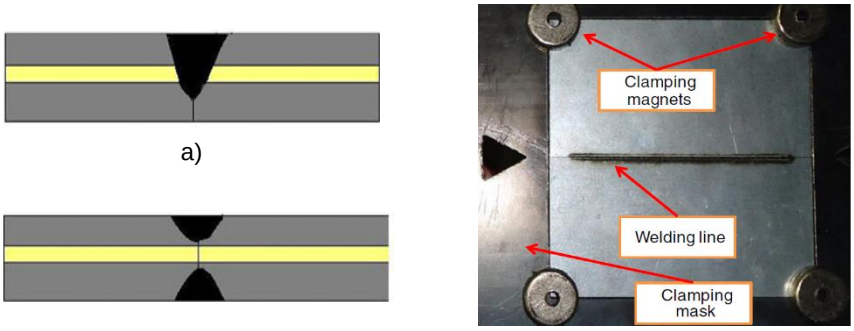

Figure 2.19 - Laser welding of sandwich composite panel, a) one-sided approach, b) two-sided approach c) real welded part (two-sided approach) [53]

The main advantages and disadvantages of LBW process are listed in Table 2.5.

Table 2.5 –Main advantages and disadvantages of LBW for joining steel-polymer sandwich composites.

Advantages	Disadvantages
• Possibility to create butt joints and therefore prevent stress concentrations, thick sections and increasing weight savings • Highly efficient technique with comparatively small heat input. • Easily automated	• Risk for polymer degradation due to high heat input of the process • Cracking susceptibility of thin materials due to high cooling rates causing large stresses (laser spot weld) • High cost of the laser equipment • Strict joint accuracy requirements

- **Friction stir welding**

Friction stir welding (FSW) is a solid-state joining process meaning that there is no molten state included in the welding process [54]. The welding process proved to be suitable to produce joints between MPM panels and a solid metal object or another MPM panel.

In an FSW process, welded metallurgical bonds are formed between the metal sheets by the use of a non-consumable tool, the friction stir weld tool. The tool is characterized by a round shank with an axially extending end with a smaller diameter, the probe. The tool rotates and is pressed into the MPM panel, the probe firstly penetrates the first sheet, followed by local displacement of the encountered portion of polymer and penetration of the second sheet. The friction between the rotating tool and the contacted metal locally heats the workpiece to momentarily soften, plasticize, and stir the metal. The basic principle of FSW process as well as the identification of the main process players is illustrated in Figure 2.20 a). Figure 2.20 b) and c) shows two material pairings of composite sandwich panels joined by FSW process.

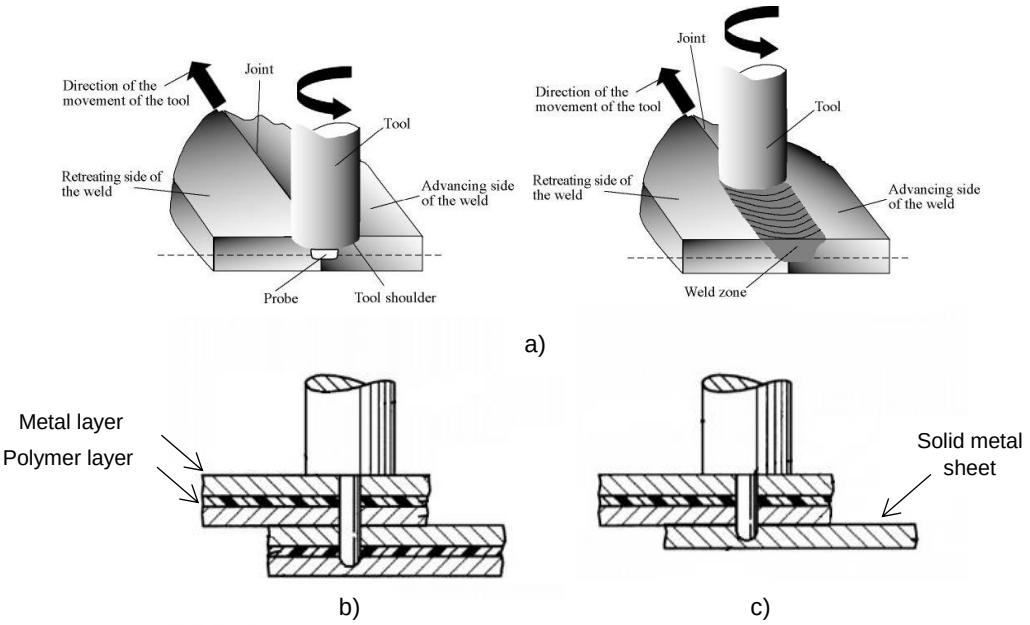

Figure 2.20 - FSW process: a) Principles of the process and nomenclature used, [55]; b) Schematic cross-sectional view of two MPM panels joint and c) MPM panel - metal sheet joint [56]

The main advantages and disadvantages of FSW process are listed in Table 2.6.

Table 2.6 - Main advantages and disadvantages of FSW for joining steel-polymer sandwich composites.

Advantages	Disadvantages
• Safe welding process. • No consumable, no filler metal and no shielding gas is required in this process. • "Green" technology as it does not produce any environmental or health hazard materials. • No surface preparation is required.	• Heavy duty clamping setup is required to hold the workpiece during welding process. • Large downward forces of the probe tool. • Long joining times • Initial cost of the FSW machine is too high. • Less flexible than arc welding processes

2.2.3. Mechanical joining

In mechanical joining there are two major categories: (1) mechanical fastening, and (2) mechanical attachment [57]. Both rely exclusively on the use of physical interlocking at a macroscopic or microscopic level, or both, to hold parts together. The greatest advantages of mechanical joining are that it can be accomplished without changing the composition or structure of material comprising parts.

2.2.3.1. Mechanical fastening

Mechanical fastening is the dominant technology for joining metal-polymer sandwich composites and the application is the same as in solid panels, a supplemental device is used to cause the interlocking between parts. The resulting joints are easily assembled and disassembled without damaging the sandwich composites – non-permanent joints.

- **Screws or Rivets**

The major concern in mechanical fastening of metal-polymer panels using screws or rivets is their notch sensitivity that may lead to crack initiation during drilling of the hole. Crack initiation in this stage may cause premature failure of the joint. Also, it must be ensured that the local compressive stresses in the joint zone do not cause critical retardation effects (creep) in the polymer core, resulting in a loss of preload in the riveted or threaded connection due to joint element relaxation. The mechanically fastened joint is also sensitive to creeping under thermal stresses.
The main advantages and disadvantages of mechanical fastening process are listed in Table 2.7.

Table 2.7 - Main advantages and disadvantages of mechanical fastening for joining steel-polymer sandwich composites.

Advantages	Disadvantages
• Easy disassembly of the joining parts • Capability of joining dissimilar materials • Joint inspection is easy • Failure predictability	• High stress concentration at the fastening points • Non-continuous joint that allows diffusion of moisture, fluids, etc • Intensive labour involved • Overlap joints leading weight penalties • Increased cycle times due to pre-drilling of holes

- **Self-pierce Riveting**

Self-pierce riveting is a cold joining process, variant of mechanical fastening process, that was also developed to join MPM sandwich panels [58].
Self-pierce riveting (SPR) is a high-speed mechanical fastening process for point joining sheet material, typically steels and aluminium alloys. It is a single-step technique, generally using a semi-tubular rivet to clinch the sheets in a mechanical joint. Pre-drilled holes are not required, allowing the joint to be made rapidly in one operation. The process cycle is shown in Figure 2.21.

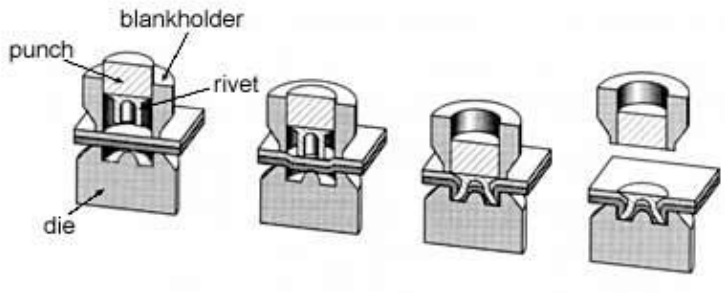

Figure 2.21 - Step sequence of the self-pierce riveting process [59]

The process starts by clamping the sheets between the die and the blank holder. The semi-tubular rivet is driven into the materials to be joined between a punch and die in a press tool. The rivet pierces the top sheet and the die shape causes the rivet to flare within the lower sheet to form a mechanical interlock, consequently a button is formed on the underside of the lower sheet.

As MPM sandwich panels are intended predominantly as replacement materials for body panel applications, SPR is investigated as a viable volume manufacturing process for joining these materials to other body parts.

One example already investigated concerns joining Hylite®, an aluminium-polymer sandwich panel, with aluminium sheet, as shown in Figure 2.22. Key parameters of the process are the setting force, dimension of the rivet and dimension and profile of the upsetting die.

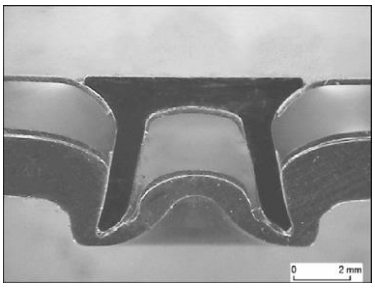

Figure 2.22 - Self-pierce riveting joint Hylite®-aluminium [58]

The main advantages and disadvantages of SPR process are listed in Table 2.8.

Table 2.8 - Main advantages and disadvantages of SPR for joining steel-polymer sandwich composites.

Advantages	Disadvantages
• Fast, single operation joining process • No fume, no spark and low noise • Ability to join similar and dissimilar materials • No surface pre-treatment required • No requirement for pre-drilled/punched holes and alignment.	• Two-side access required • A joint button left on one side • Additional cost and weight from the rivet • . Possibility of galvanic corrosion between the steel rivets and the aluminium alloy substrate, unless corrosion protective coatings are used on the rivet surface. • Relatively high rivet insertion force required.

2.2.3.2. Joining by forming – Hemming processes

Joining-by-forming is a type of mechanical attachment joining method where joining is accomplished by a mechanical interlocking created through forming operations between designed-in geometric features integral to the parts being joined. No supplemental devices are needed to perform the joint. Its application to metal-polymer sandwich composites is nowadays limited to robotized hemming processes such as Table-top hemming and Roller hemming.

Both processes are commonly used in the assembly production of closures (opening parts like doors, hoods, trunk lids and roofs) and they can be implemented to Litecor® parts virtually without adapting the conventional process; only the Table-top hemming process requires a minor modification. They consist in joining two sheet metal parts by plastic deformation where a metal sheet edge of an outer part is bent around an inner part by hemming to create a hem. No consumables are used such as screws, rivets or adhesives and hence no extra weight is added.

- **Table-top hemming**

A Table-top hemming process is a three-step process which includes the following three steps, 1. Bending or flanging, 2. Pre-hemming and 3. Finish hemming, as illustrated in Figure 2.23.

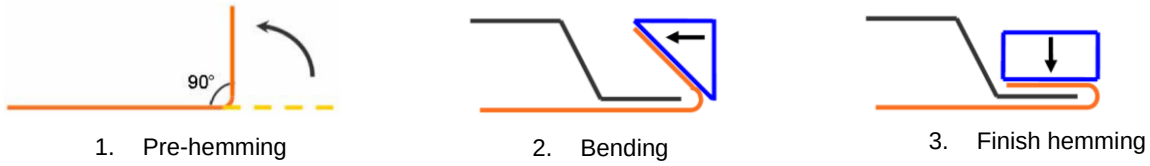

Figure 2.23 - Scheme of the Table-top hemming process [60]

The main process variables are “hemming force” and “force holding time” for each step process. In hemming operations, some of the bending radii occurring are very small, causing extreme compression of the inner face sheet and stretching of the outer face sheet.

Due to the material’s high stiffness, special adaptations are required for the Litecor® composite to achieve a flawless hemmed joint, Figure 2.24. When applying this process to Litecor®, there is a risk of cracking of the outer fibres. To avoid it, ThyssenKrupp has developed an effective solution for Table-top hemming based on a geometric adaptation which consists in the formation of a groove in the bending die to specifically influence the material when bending the outer panel. The groove leads to the formation of a defined, softer area in the inner fibres during bending. This groove enables longitudinal compensation in the inner fibres during the first hemming step so that the tensile fibres are relieved in the outer hemming process and therefore avoids crack formation.

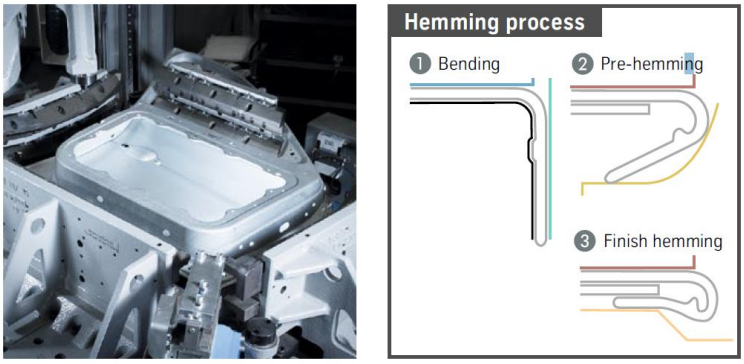

Figure 2.24 - Hemming system and process steps for the new Table-top hemming process [36]

Besides the geometric adaptations for the pre-hemming operation, it is essential to have a precise control of the process hemming force with holding time in the finish hemming position. By doing this, the body parts can be hemmed with constant quality and without cracking within the usual body shop cycle time.

Process consistency for hemming Litecor® was verified on this newly developed Table-top hemming system which is suitable for use in volume production.

The main advantages and disadvantages of Table-top hemming process are listed in Table 2.9.

Table 2.9 - Main advantages and disadvantages of Table-top hemming for joining steel-polymer sandwich composites.

Advantages	Disadvantages
• High product quality • Good aesthetic • Reduced cycle time • Suitable for high volume production and easy to integrate on an assembly line.	• High investment level - the whole installation is product specific. • Compact joint but with lower strength than welded joints

- **Roller Hemming**

In robot roller hemming the hem is created by a different movement pattern. A robot guides a roller parallel along the flange which bends the outer part around the inner part. The geometries and diameters of the rollers can vary according to the process application. The process steps of a robot roller hemming process are depicted in Figure 2.25 a) and b). The edge of the outer part (grey) is bent in three hemming steps in sequence. In between the hemming steps the orientation of the roller is switched.

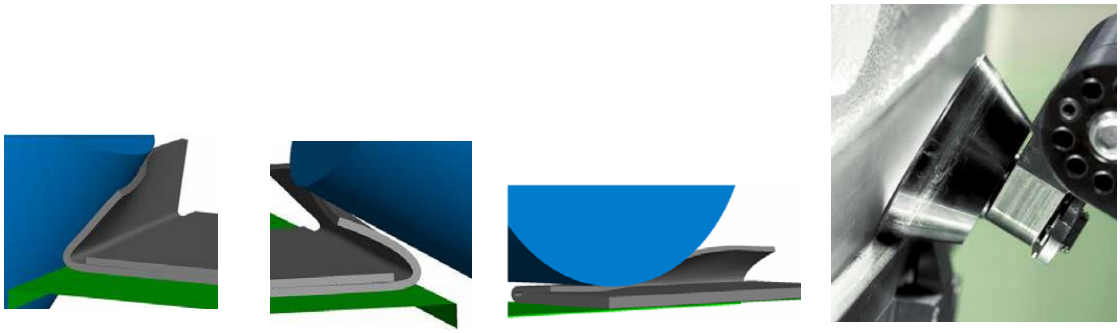

a) b) c)

Figure 2.25 - Roller hemming steps: a) Two pre-hemming steps; b) Final hemming step [60] c) Roller hemming Litecor® [30]

In roller hemming process, a common undesirable quality problem is the waviness along the flange [60]. To avoid the phenomena, the process parameters must be selected carefully, and, in some cases, further roller passes may be necessary for smoothing the joint.

The studies of the application of roller hemming processes to Litecor® composite parts were undertaken using the example of the door outer panel but can also be transferred to other outer panel components such as the hood, trunk lid or roof. A hem from Litecor® outer skin created by roller hemming is shown in Figure 2.25 c).

The main advantages and disadvantages of roller hemming process are listed in Table 2.10.

Table 2.10 - Summary of the main advantages and disadvantages of roller hemming for joining steel-polymer sandwich composites.

Advantages	Disadvantages
• Low investment lever for each new product: the equipment can be simply re-programmed for other products • High product quality • Good aesthetic • More simple and economic that Table-top hemming • More flexible	• Increased cycle time - application to low and middle volume production. • Compact joint but with lower strength than welded joints

2.3. Joining by forming – Mortise-and-tenon joints

The traditional mortise-and-tenon joint, has been used for thousands of years by carpenters and blacksmiths to simply attach wood parts or join metal parts by hot forging, examples of applications are shown in Figure 2. 26.

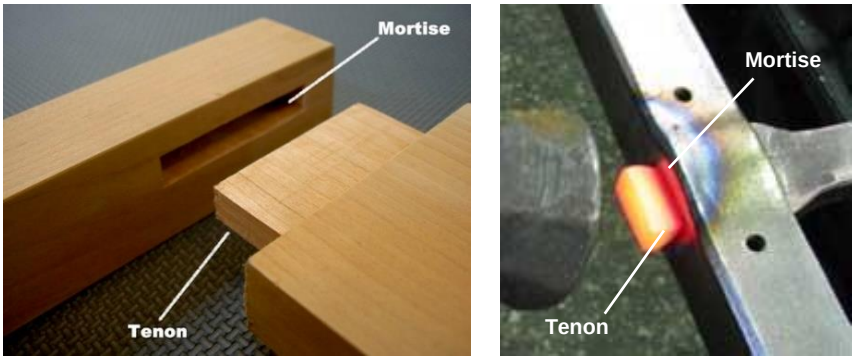

Figure 2.26 - Traditional mortise-and-tenon used to: a) simply connect parts [61]; b) join metal parts [62]

Recently investigations developed by Bragança et. al [63,64] focused on creating mortise-and-tenon joints by sheet-bulk metal forming (SBMF) processes, between monolithic materials.
SBMF processes are defined as forming of sheets (or plates) with intended three-dimensional material flow as in bulk forming processes. The class of SBMF processes is based in forming processes in which often conventional sheet and bulk forming operations are combined, encompassing plastic flow under plane-stress or three-dimensional stress conditions, respectively [65].

SBMF processes is used mostly for the fabrication of sheet metal parts, however it has great potential to be applied for the joining sheets (or plates), being classified as a joining by forming process. In most cases the intention of the sheet-bulk metal forming processes is to form local shape elements with dimensions with the order of magnitude of the sheet thickness, projecting out of the plane of the sheet. As a result, the dimension of the resulting functional elements can be locally increased, decreased or remain equal in comparison to that of the original specimen depending on the tool motion of the sheet-bulk metal forming process [65].
From a production engineering point of view, SBMF requires single or combined application of loading by tools across and/or perpendicular to sheet thickness [66]. The directions across and perpendicular to sheet thickness are designated as ‘S’ (across), ‘T’ (transverse-perpendicular) and ‘L’ (longitudinal-perpendicular) in Figure 2.27.

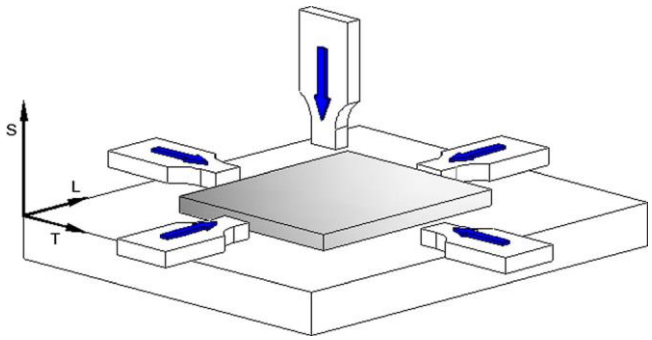

Figure 2.27 - Loading directions in sheet-bulk metal forming (SBMF) processes [66]

The joining solution developed by Bragança et. al is based on a variant of the traditional 'mortise-and-tenon' joint, previously described. This time instead of simply connecting the parts, or join metal parts by hot forging the tenon, the 'mortise-and-tenon' can be used to produce locked joints where the mechanical lock is ensured with one cold forging operation: end compression through the tenon, in a direction perpendicular to the sheet thickness ('T' and 'L' directions of SBMF in Figure 2.27).

The process revealed good preliminary results for joints composed of aluminium plates, making it possible to try other applications, such as hybrid connections – aluminium and polycarbonate, Figure 2.28.

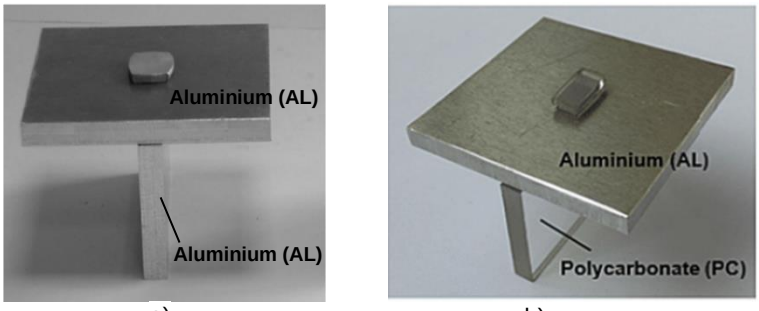

a) b)

Figure 2.28 - Mortise-and-tenon joint to lock parts: a) Al-Al joint [63]; b) Al-PC joint [64]

The potential of SBMF in applications of joining-by-forming [67] to join MPM sandwich materials have not yet been addressed in the literature.

This work thesis is then focus in the application of this type of joining processes and variants thereof, with more than one forging operation, to join metal-polymer sandwich composite panels.

3. Process description and modelling

The joining processes under investigation to join Litecor® sheets perpendicular to one another were designed from scratch. The joining processes design considered several factors such as: geometry and dimensions of the joining elements, designing or selecting the most appropriate tools for the operation to achieve the intended deformation and joint interlocking, the choice of process parameters and the selection of the machine tool. Throughout this chapter and the experimental development chapter, these aspects will be analysed for each joining process developed.

This chapter is divided in two subchapters. The **first subchapter** concerns a detailed description of the whole joining processes to be carried out, describing the stages involved, the tools used, and the relevant geometric properties of the different stages. The **second subchapter** introduces the numerical modelling supporting the joining by forming processes under investigation to join MPM sandwich panels.

3.1. Description of the new proposed joining by forming processes

The joining by forming processes developed are variants of the mortise-and-tenon joint previously described, that is specifically developed to fix two perpendicular composite sandwich panels longitudinally in position. The goal is to produce a purely mechanical joint locked exclusively by plastic deformation of the material constituents without resorting to any type of consumables or external components (screws or rivets, for instance).

All joining processes were developed to join MPM sandwich panels perpendicular to one another using the same workpiece/specimen. It consists in a unit-cell which replicates the mortise-and-tenon joints utilized for fixing longitudinally in position two sandwich composite panels perpendicular to one another in a T-shaped joint configuration, Figure 3.1 a). It is composed of two elements, a small sample with a tenon (the first element), which is longer than wider and another small sample with a mortise (second element) consisting of a rectangular through-thickness hole. Figure 3.1 b) represents the unit-cell in which two sandwich composites sheets made from the same material with equal thicknesses t are assembled by connecting the tenon with the mortise resulting in the dimensions of l_t and w_m, free-length of the tenon and width of the mortise, respectively. The cross-section of the unit-cell is also schematically represented in Figure 3.1 c); it shows the skin layer thickness dimension t_s and the core layer thickness t_c of the metal-polymer sandwich panel as well as the slight clearance j between the tenon and the mortise intentionally designed to facilitate sheet assembly.

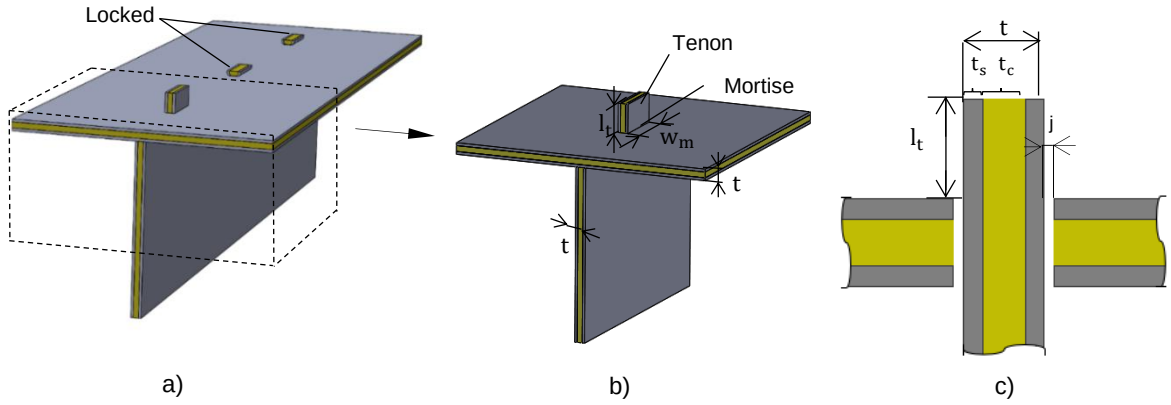

Figure 3.1 - Schematic representation and terminology for a) fixing longitudinally in position two sandwich panels perpendicular to one another in a T-shaped joint configuration b) unit-cell considered for the proposed joining processes development c) cross-sectional view of the tenon-and-mortise elements of the unit-cell

The three joining processes can be classified as joining by forming processes, a mechanical joining subcategory, in which joining is accomplished by a mechanical plastic interlocking between designed-in geometric features integral to the parts being joined using forming processes.

The mechanical lock of the joints is created through local plastic deformation of the free-length of the tenon l_t and the width of the mortise w_m. A close observation to Figure 3.2 allows to conclude that the tenon acts like a rivet. The smooth head end of the rivet is replaced by the connection of the tenon to the surrounding material of the sheet, mortise, and the opposite free-length of the tenon (hereafter designated simply as 'free-length'), Figure 3.2 a), is upset by a certain sequence of compression operations according to the joining process stages to produce a flat-shaped surface head. These dimensions will dictate the protrusion of the joints (visual aspect) and will have implications in their strengths, see Figure 3.2 b).

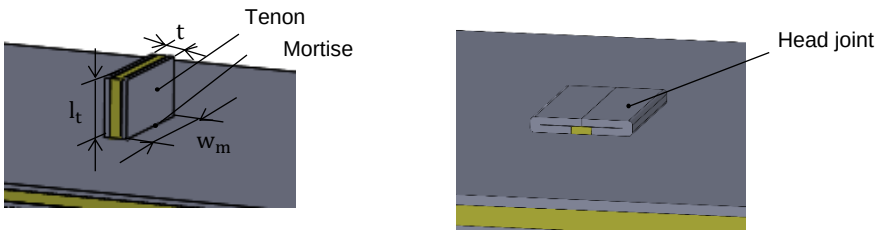

Figure 3.2 - Joining process dimensional nomenclature: a) Before the joining test – mortise-and-tenon b) After the test – head joint

The three joining by forming process designs draws from an earlier development of Bragança et. al. to join monolithic sheets (metal and polymer) by sheet-bulk metal forming, to new solutions based on multi-stage forming sequences that are more appropriate for sandwich composites. The name given to each one of them considers the total number of stages. They differ in deformation design concept, number of total operation stages and in the die usage.

3.1.1. Single-stage joining process

As the name suggests, the joint can be described in one single operation:

1. **Upset compression**: the single-stage joining process consists in an open-die compressive forming operation named upset compression. In this process a flat punch applies a vertical load F on the tenon, in the direction perpendicular to its thickness to plastically deform its free-length l_t, and ensure a mechanical interlocking between the two sandwich composite panels to be joined by the formation of a sound flat-shape head. (Figure 3.3). The 2D dimensions of the final head, length l_h and thickness t_h, are dependent on the level of compression dictated by the punch displacement d.

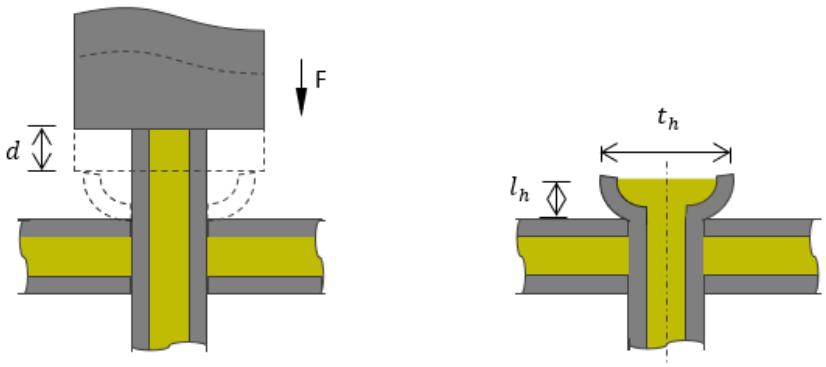

Figure 3.3 - Schematic representation of the single-stage joining process

This is a process subject to Euler macro-buckling failure, hereafter referred simply as buckling failure. This type of failure consists in a plastic instability of the material characterized by a wavy condition of the workpiece caused by compressive stresses.

This thesis studies a new application of this process: to join sandwich composite materials (metal-polymer panels) instead of monolithic materials.

The second and third joining processes were specifically designed to avoid the buckling failure during the joining process and are the new solutions based on multi-stage forming sequences intentionally developed for sandwich composites.

3.1.2. Two-stage joining process

The second design concept is an innovative two-stage joining-by-forming process that intends to impose stable plastic deformation conditions and thus reverse the probability of buckling occurrence as well as produce larger flat-shaped heads, focusing on increasing the head thickness t_h. It combines the following two stages:

1. **V-shape indentation:** In the very first stage, a V-shape indenting operation is performed with the aid of a V- punch applying a vertical load F. The geometry of the V-punch die used is designed so that at the end of the operation the tenon is divided into two halves by the opening of a groove in the core layer of the tenon. The V-punch is characterized by its included angle θ and has a displacement d. As a result of such indentation, the metal skin layers are forced to bend outwards moving away from the tenon's axis of symmetry as represented in Figure 3.4. After this stage, the two portions of material divided for each side of the V-punch faces are recognized as

flanges. The opening of the groove and consequently the separation of the flanges is strictly dependent on the V-punch parameters θ and d.

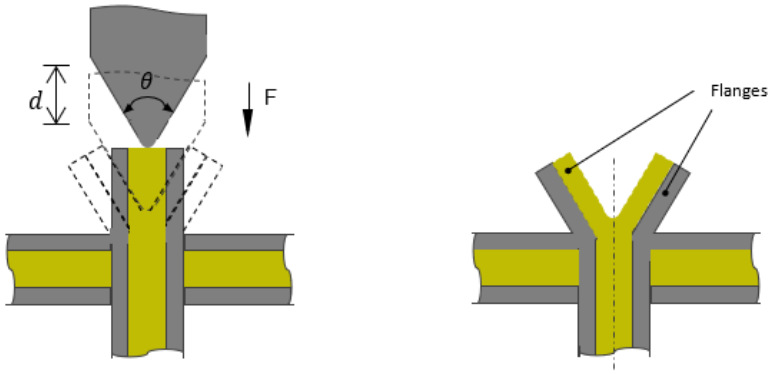

Figure 3.4 - Two-stage joining-by-forming process: schematic representation of the V-shape indentation stage.

2. **Upset compression:** In the second stage, a flange forming operation is performed. The flanges are forced to fully outer bend by upset compression using a flat punch with downward linear motion in the direction perpendicular to sheet thickness. The flat punch applies a given force F travelling a certain displacement, d. The flanges bend over the mortise here acting as the matrix of the bending process. The flange opening angle β, is 90º (Fig. 3.5). The 2D dimensions of the final head, length l_h and thickness t_h, are dependent on the level of compression dictated by the punch action.

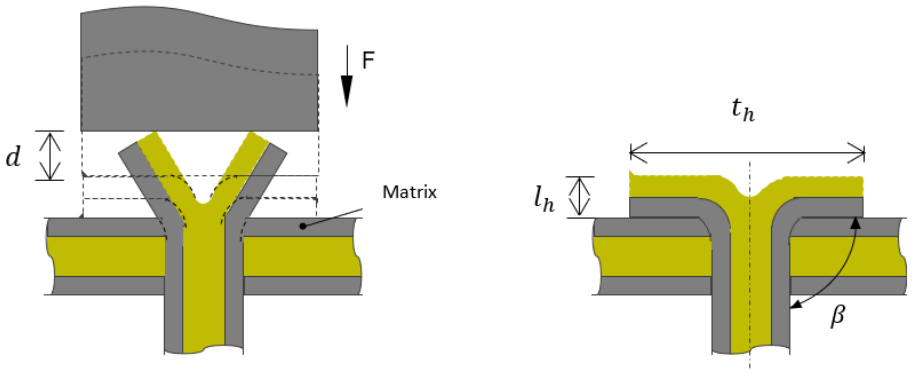

Figure 3.5 - Two-stage joining-by-forming process: schematic representation of the upset compression stage.

3.1.3. Three-stage joining process

The third design concept is a new proposed three-stage joining-by-forming process. Like the two-stage joining process, this one was also developed to avoid the buckling occurrence but with this process the goal is to be able to produce joints with increased flat-shaped heads by adding a compression bead. It is composed by the following three stages:

1. **Cutting:** The first stage requires the removal of the polymer core layer of the tenon. The volume removed corresponds to the volume placed above the surface line of the mortise. The polymer core

layer is cut out using a saw blade rotating at ω as illustrated in Figure 3.6. In the end of the cutting stage, the isolated skin layers are called flanges.

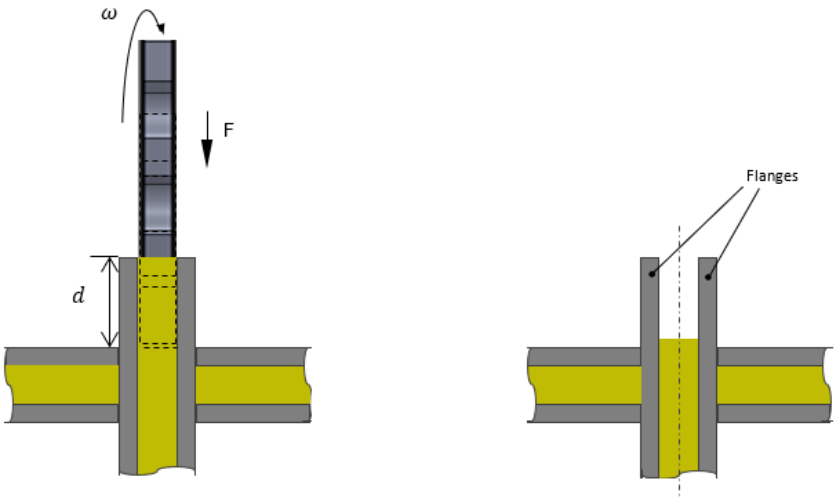

Figure 3.6 - Three-stage joining-by-forming process: schematic representation of the cutting stage

2. **Nosing:** In the second stage occurs a flange forming operation named Nosing, where the flanges are forced to inner bend by the linear motion of a U-concave punch that applies a given load F. The curving of the flanges occurs gradually towards the centre of the tenon until its inner edge tips touch each other in the tenon's axis of symmetry as shown in Figure 3.7.

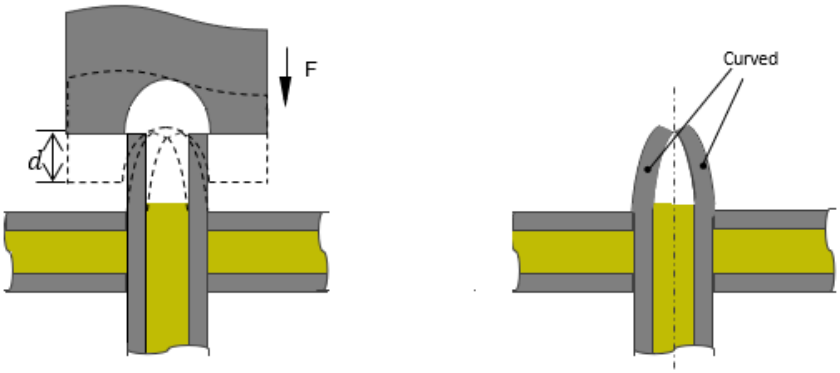

Figure 3.7 - Three-stage joining-by-forming process: schematic representation of the nosing stage.

3. **Upset compression:** In the third and final stage, the curved flanges will undergrow an open-die compressive forming operation named upset compression. A flat punch applies a vertical load F and as the punch moves downwards, the flanges will deform until it reaches the final shape illustrated in Figure 3.8.

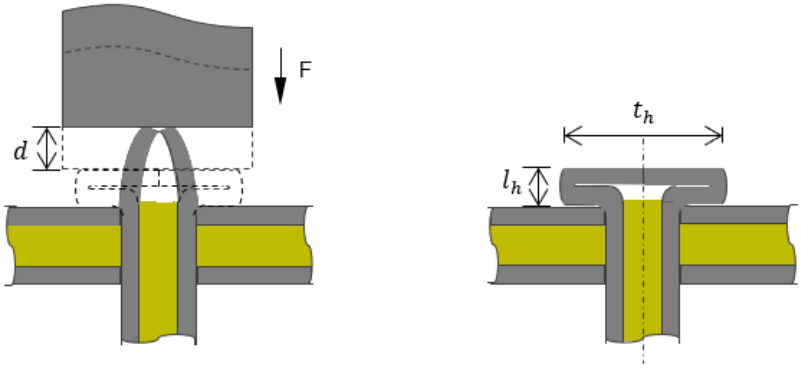

Figure 3.8 - Three-stage joining-by-forming process: schematic representation of the upset compression stage.

The three joining-by-forming processes investigated are compiled in a schematic representation illustrated by Table 3.1.

Table 3.1 - Overview on the three joining-by-forming processes under investigation, stages with respective dies.

Joining process designs			
Design concept #1	Single-stage		
	1 – Upset compression		
	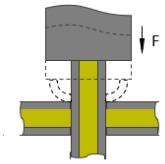		
Design concept #2	Two-stage		
	1 – V-shape indentation	2 – Upset compression	
	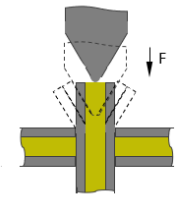	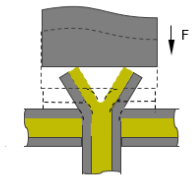	
Design concept #3	Three-stage		
	1 – Cutting	2 – Nosing	3 – Upset compression
	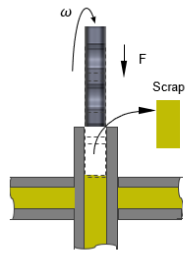	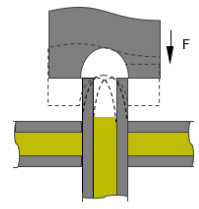	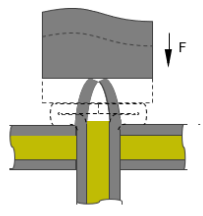

3.2. Numerical modelling

The goal of using numerical modelling is to increase process know-how and compensate the gap of technological practice in the development of the new proposed joining processes.

In this study, the numerical simulations performed are useful for two main reasons:

First it allows to evaluate the physical feasibility of the joining processes by obtaining a very realistic forecast of the process to be performed, predicting the material flow during plastic deformation in each step of the process. The geometry of the material and/or the tools used can be optimized to improve the flow of material. In this way, the experiments to be performed can be simplified in terms of cost and time spent, being more easily optimized.

Secondly, it allows to validate the joining processes with higher safety by comparing the data obtained in the numerical simulations to the one obtained through laboratory experiments. These data are presented in a graphical format to facilitate the understanding of the different steps of the joining process according to the evolution of force vs punch displacement.

- **Software**

The numerical modelling of the joining by forming processes was carried out with the in-house finite element computer program *I-FORM* [68]. The software allows solving problems associated with plastic deformation using finite element method and plasticity theory [69], both in bi-dimensional deformation methods (plane strain, plane stress or axisymmetric) and tri-dimensional.

- **Modelling conditions**

The numerical simulations performed used two-dimensional finite element models under plane strain deformation conditions, which means that the width of the material w_t is modelled as a constant during the plastic deformation in every numerical simulation performed.

The cross-section of the sandwich composite panels was modelled as deformable objects and were discretized by means of quadrilateral elements. The clearance j between the tenon and the mortise was assumed to be 2.5% of panels' thickness in each side, Figure 3.9 b).

According to mesh refinement, two sections can be identified in the simulations. Section A is the section where the major plastic deformation will occur and therefore the mesh is refined in this section. Section B corresponds to the area where it is predicted that the material will not undergo significant plastic deformation and that is why the mesh was kept unrefined, Figure 3.9 a).

The material of each material layer (steel and polymer) was defined according to the corresponding flow curve, true-stress vs true-strain, provided by the mechanical characterization tests carried out.

The modelling of contact between deformable objects was needed in the numerical simulations performed and considered a penalty-based algorithm for avoiding self-penetration of an object or penetration of one object into another. A friction factor was also considered between objects. The friction model used was the Prandtl friction model. No thermal influence was introduced, because the test is carried out at room temperature.

The set of dies used is also represented in Figure 3.9 a). Although these are not physically identical to those used in the experiments, they were modelled in such a way that their action and constraint are

like what was verified experimentally, thus ensuring a concordance between both methods of analysis. They were modelled as rigid objects and their geometries were discretized by means of linear contact-friction elements.

The simulation time was less than 5 min, depending on the free-length of the tenon and the type of joining process performed.

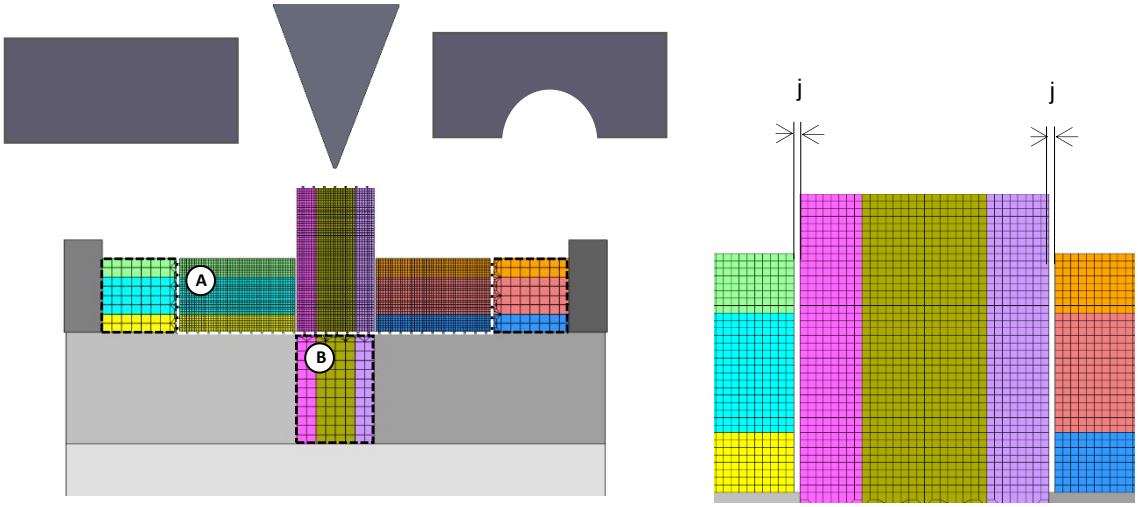

a) b)

Figure 3.9 - Numerical modelling: a) initial mesh and simulation layout for a Joining test ($l_t = 2\ \mathrm{mm}, nº\ \mathrm{elements}: 5488$) b) zoomed section, highlighting the clearance j.

4. Experimental development

This chapter presents the experimental work that was carried out to perform the joining-by-forming processes described in chapter 3.

The experimental work was performed in partnership with the scientific area of Mechanical Technology and Industrial Management, belonging to Instituto Superior Técnico and encompasses a series of experimental tests.

To address all relevant points of the experimental work, this chapter is divided in three sub-chapters. The **first subchapter** lists the sequence of experiments carried out. The **second subchapter** presents the set of equipment used throughout the experiments. Finally, the **third subchapter** describes all experimental procedures performed in each test category, namely material characterization test, joining tests, preparation of the test specimens, the tools used, and the major process parameters and destructive tests performed on all the joints obtained.

4.1. Overall experimental plan

The overall experimental plan was structured in three main test categories as shown in Table 4.1. First, two material characterization tests were performed, one to reveal information about the mechanical properties of the material under investigation and the second to determine the buckling conditions of a Litecor® column under compressive loading. After that, each joining processes were tested to investigate their capability to join Litecor® steel-sandwich panels: the single-stage, the two-stage and the three-stage joining process. Finally, the performance of the produced joints was tested by means of destructive tensile pull-out tests aiming to determine the force to detach the two panels and investigate the corresponding failure mechanism.

Table 4.1 – Overall experimental plan

Test category / Material and its condition		#1 Material tests		#2 Joining by forming tests			#3 Destructive test
Material	Treatment	Mechanical characterization test	Instability test	Single-stage joining process	Two-stage joining process	Three- stage joining process	Tensile pull-out test
Litecor®	As-received	✓	✓	✓	✓	✓	✓

4.2. Equipment

The set of equipment used throughout the experiments is illustrated in Figure 4.1.

The water jet cutting machine used is a FLOW waterjet MACH3-4020B [70] shown in Figure 4.1a). It has a cutting speed of 12.7 m/min and dimensions of 4 m x 2 m. A water jet cutter is a high precision cutting machine which uses a high-pressure jet of water, or a mixture of water and an abrasive substance to cut a variety of materials.

The hydraulic press is an INSTRON, SATEC 1200, shown if Figure 4.1 b). A hydraulic press is a machine that uses a hydraulic cylinder to generate axial force. SATEC 1200 has a maximum capacity of 1200

kN and it is incorporated with a software that allows to carry out tests of upward movement (tensile tests) and downward movement (compression tests). The load cell of the press measures the load exerted during the test, while the displacement transducer measures the existing vertical displacement.

The universal testing machine INSTRON 4507 was also used during the experiments. It offers a maximum capacity of 200 kN and a maximum actuating speed of 500 mm/min. This type of testing machine is used to test tensile and compressive strengths of materials, it is also possible to perform bending tests.

All the equipment used belongs to the Manufacturing & Process Technology Laboratory [71], [72] except the waterjet that belongs to an external company, 4x4 Multitrabalhos Lda.

a) b) c)

Figure 4.1 - Equipment used in the experimental procedures: a) Waterjet cutting machine b) Hydraulic press c) Universal testing machine

4.3. Experimental procedures

In this subchapter the material under investigation and the experimental procedures concerning each test category of Table 4.1 will be presented.

4.3.1. Material

Ten Litecor® panels were supplied by ThyssenKrupp company itself as samples to be tested with dimensions of ($LxWxt$)=(50x30x2) mm and symmetrical structure with thickness dimensions of (t_s / t_c / t_s) = (0.50/1.0/0.50) mm. t_s – skin layer thickness and t_c – core layer thickness. The dimensions mentioned are illustrated in Figure 4.2. These panels were the starting point for the different experimental tests performed.

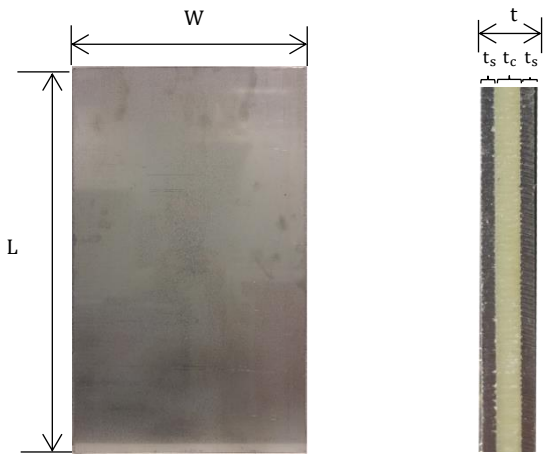

Figure 4.2 - Dimensions of the Litecor® panels received by ThyssenKrupp; a) Litecor® sheets; b) sheet thicknesses in a cross-section view

4.3.2. Mechanical characterization test

To find the mechanical properties of Litecor®'s material constituents (steel and polymer), the mechanical characterization test performed was the stack compression test [73]. The goal is to draw flow curves in true stress vs true strain for both materials. The stack compression test is a compression test performed on stacked multi-layer cylinder specimens.

- **Specimen preparation**

In total, four specimens were metallography prepared, two for each material constituent of Litecor®. The geometry of the specimens used is shown in Figure 4.3. They are formed by stacking up discs machined out from Litecor® sheets in the as-received condition. The main dimensions are its height (h_0) and its diameter (D_0).

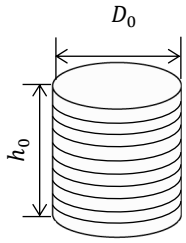

Figure 4.3 - Geometry of the cylindrical specimen used in stack compression tests

The Litecor® panel was milled in a vertical milling machine to i) isolate the steel sheet by progressively removing the first steel sheet and the polymer layer, ii) isolate the polymer layer by removing the two steel skin layers. After that, the steel discs were produced using a hole-saw cutter mounted on the pillar driller, while the polymer ones were made with a hollow punch tool. Figure 4.4 shows the sequence mentioned above. The steel discs were then machined in the lathe to the intended diameter D_0.

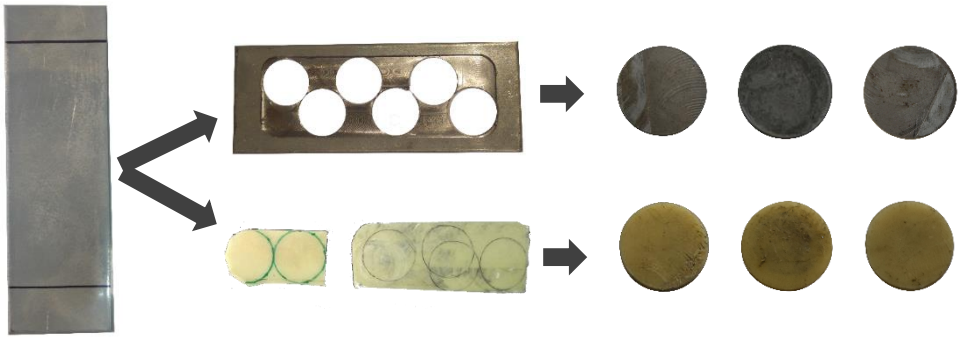

Figure 4.4 - Sequence of procedures to obtain steel and polymer discs from the Litecor® panel.

The steel and polymer discs were then stacked by pilling up the discs to form a layered cylinder. Glue lines were applied on the outer surface of the cylinder to create final multi-layer cylindrical specimens for steel and polymer. The specimens produced, and their dimensions are shown in the Table 4.2.

Table 4.2 - Dimensions of the stack compression specimens

Steel	Before test		Polymer	Before test	
Specimen 1	$D_0 = 14.07$		Specimen 1	$D_0 = 14.07$	
	$h_0 = 8.20$			$h_0 = 8.20$	
Specimen 2	$D_0 = 14.21$		Specimen 2	$D_0 = 14.18$	
	$h_0 = 8.30$			$h_0 = 8.55$	
Dimensions in mm					

- **Procedure**

The stack compression test was carried out in the hydraulic press with a cross-head speed equal to $5\ mm/min$. Graphite grease lubricant was used in the upper and lower flat punches aiming to minimize the friction in tool-specimen interface.

To draw the true stress-strain curves, it was necessary to convert the output data of the stack compression tests from force vs displacement data to true stress vs true strain data, as follows:

- True strain, $\bar{\varepsilon} = ln\frac{h_0}{h_i}$ (4)

  With:
  - $h_i = h_0 - d$, at time *i*;
  - $d =$ punch displacement.
- True stress, $\bar{\sigma} = \frac{F_i}{A_i}$ (5)

  With:
  - A_i calculated by volume conservation:
    - $V_i = V_0 \Leftrightarrow A_i = \frac{V_0}{h_i} \Leftrightarrow A_i = \frac{A_0.h_0}{h_i}$

The results were retrieved averaging the data obtained from the two specimens for each material and presented in the same chart for better comparison comprehension, as shown in Figure 4.5. It shows that the mechanical properties relevant for joining the Litecor® sheets by forming of the sandwich material

are primarily determined by the steel face sheets. Their strength is much higher than the polymer core layer.

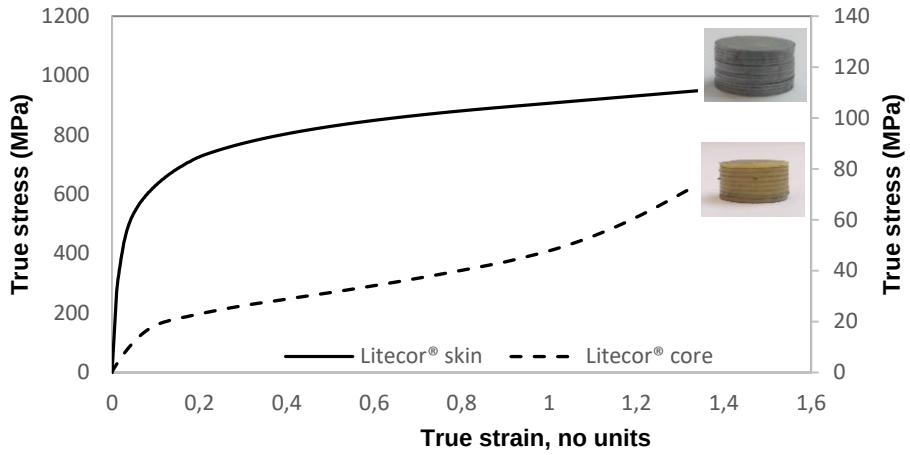

Figure 4.5 - True stress-strain curves of Litecor®'s constituent materials. Note: The left vertical axis applies for the steel and the right vertical axis applies for the polymer.

4.3.3. Instability test

The instability test was performed to investigate the buckling conditions of Litecor® by determining the range of length dimensions for which the upset compression of a Litecor® column can be performed without signs of plastic instability and failure by out-of-plane buckling.

- **Specimen and Laboratory tool**

The specimen used for the instability test consists in a rectangular column cut from the Litecor® panels received. To obtain different tenon lengths they were milled in the vertical milling machine until obtain the intended free-length, l_0.

The laboratory tool in which the instability test was performed consists in a stainless-steel cylinder block with a rectangular feature in the centre. Figure 4.6 presents a schematic representation and photos of both the specimen and the tool used in the instability test.

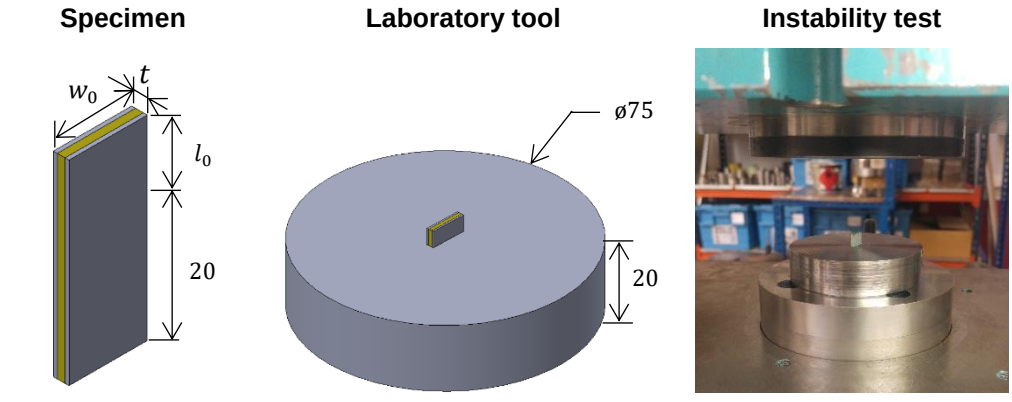

Dimensions in mm

Figure 4.6 - 3D model and photograph of the specimen and tool used in the instability test

- **Procedure**

The specimen is mounted in the tool being cantilevered along the 20 mm length of the tool. The remaining length of the tenon is the free-length l_0 and it will undergo upset compression using a flat punch, the test is performed at room temperature in the hydraulic press over displacement control with a constant vertical velocity equal to 5 mm/min.

The instability test work plan is shown in Table 4.3 and it was defined based on the joining processes. Consecutive tests, $i = 1, \dots, n$, were carried out in which the free-length of the tenon l_{0_i} was varied by rising $0.5\ mm$ at a time. The test is finished once the critical buckling length, l_{cr}, is reached.

Table 4.3 - Experimental work plan for the instability test (nomenclature according to Figure 4.6)

Test case	Specimen	Material	$t\ (mm)$	$w_0\ (mm)$	$l_{0_i}(mm)$
Instability test	Instability tenon	Litecor®	2	10	$1.5, 2, 2.5, \dots, l_{cr}$

4.3.4. Joining by forming tests

Three joining by forming tests were performed to investigate their feasibility and workability to join two Litecor® panels perpendicular to one another in a T-shape configuration. The three joining processes differ in the number of steps (from one to three steps), in the die usage and consequently in the flow of material during plastic deformation leading to the creation of three different head joints and potentially different performances, based on joint strength.

The specimen used for the joining tests is the same one for each joining process investigated. Also, one same tool was used to fix the specimen and to perform each joining process. The joining tests were carried out at room temperature, in the hydraulic press over displacement control under a constant vertical velocity equal to $5\ mm/min$, so that the extrapolation of data can be quite precise with a high number of points.

- **Specimen**

The mortise-and-tenon unit cells were produced using water jet cutting. This cutting method has a great advantage of avoiding heat affected zone in the material, due to the small heat generation, which is absorbed by the water, this way the polymer does not suffer thermal deterioration and keep its physical integrity.

Computer-aided design (CAD) drawings from SolidWorks software were used to draw the tenon and the mortise elements with the right dimensions to be cut (Appendix A). Figure 4.7 a) shows a set of mortises and tenons cut from the Litecor® panel. The two elements after being cut, were assembled to obtain a unit-cell ready for testing, Figure 4.7 b). The overall dimension of the unit-cell is represented by the dimensions A and B. The tenon is based on an AxB panel, with A= $30\ mm$, and B= $50\ mm$. The mortise is cut in a squared panel BxB.

Only the free-length of the tenon l_t was allowed to vary, it was defined as one of the major operating parameters. The thickness of the tenon $t = 2\ mm$ is a constant that corresponds to the thickness of the Litecor® panels received. Regarding the width of the tenon w_t, say the width of the mortise w_m, it was

set as a constant value equal to five times the original sheet thickness $w_t = w_m = 5t = 10\ mm$. With a small clearance j between the mortise and tenon it is easy to assemble the two elements and form the unit-cell.

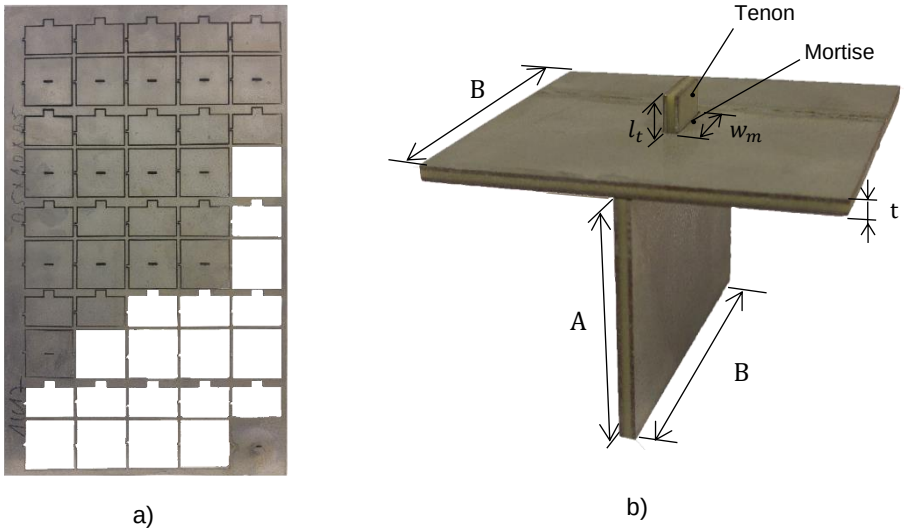

a) b)

Figure 4.7 - Manufacturing of the Joining test specimens. a) Waterjet cutting of Litecor® panels (L x W), b) Assembly of the tenon and mortise elements to form the unit-cell

- **Laboratory tool**

The laboratory tool used to carry out the joining tests has been designed considering the following requirements:

1. To have a simple geometry with the lowest components possible to facilitate its manufacture and be easily manipulated.
2. To be made of a mechanically rigid material to allow only deformation of the specimen and to prevent damage to its structure.
3. To have a safe mechanical fastening system that allows to fix the components to be deformed correctly.

A three-dimensional view of the laboratory tool with a list of its components is shown in Figure 4.9 and Table 4.4. The unit cell is mounted in a cavity formed by the central part of the laboratory tool (die segment and the two-unit cell holders). The local x_1 and x_2 axis allow moving the unit-cell holders to clamp it using M8 bolts. As seen in Figure 4.8 the mortise panel and the tenon's free-length of the unit cell are above the clamping area. The x and y-axis allow adjusting the position of the unit-cell by moving the die segment and the die shoe respectively. The tool provides one more axis, the z-axis, for loading the unit-cell perpendicular to its thickness using a punch with a rectangular section.

All components of the tool were fabricated from AISI 430 stainless steel.

Table 4.4 – Tool parts description

Nº	Part	Qty
1	Die shoe	1
2	Die segment	1
3	Unit-cell holder	2
4	Unit-cell	1
5	Punch	1

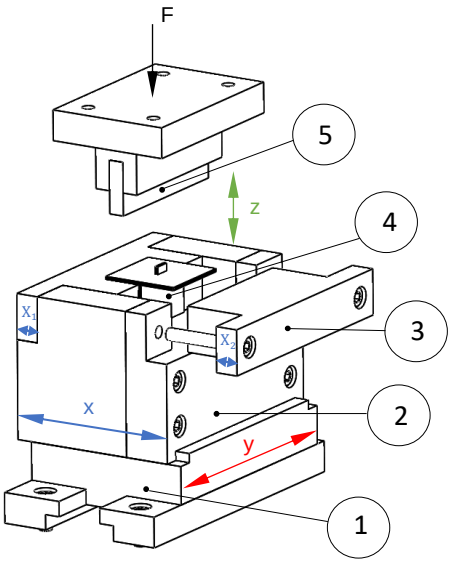

Figure 4.8 - Laboratory tool for joining a unit-cell

4.3.4.1. Single-stage joining test

The experimental work plan was defined based on instability test results and thus was possible to define the most appropriate values for the free-length of the tenon to be tested. The work plan for the single-stage joining process to connect the two Litecor® panels using the specimen "unit-cell" is summarized in Table 4.5. In total, five tests ($i = 1, \dots, 5$) were performed, the difference between them is the dimension l_{t_i}, the free-length dimension. Based on the critical free-length, $l_{t_{cr}}$, three tests were performed in the stable region and two tests were performed in the unstable region.

To perform the single-stage joining test, the unit-cell was mounted in the laboratory tool and properly fixed. The test was performed in the hydraulic press. Regarding the actuating punch it was used a flat compression punch with a displacement d_1 being set to produce a successful head joint with low protrusion which means with a head length, l_h, of a range between $0.5 - 1\ mm$.

Table 4.5 - Single-stage joining test: experimental procedure

Test	**Composite sandwich panel**	**Specimen**	**Free-length dimensions**		
Single-stage joining test	Litecor®	Unit-cell	$t\ (mm)$	$w_t\ (mm)$	$l_{t_i}\ (mm)$
			2	10	$1, 1.5, 2, 2.5, 3.5$
Stage	**Test scheme**	**Punch**	**Test apparatus**		
1. Upset compression	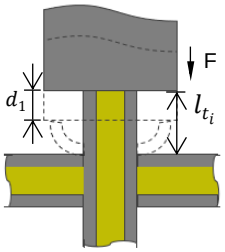	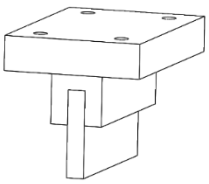	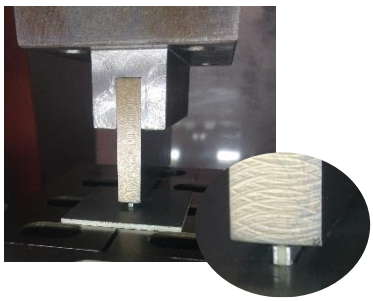		

4.3.4.2. Two-stage joining test

The two-stage joining process tested to join two Litecor® sandwich panels can avoid the buckling failure and produce head joints with increased contact area and low protrusion. The experimental work plan for this process along with the experimental apparatus of its stages is presented in the following Table 4.6. Also, five tests were performed with the same free-length initial dimensions as the single-stage joining process, to obtain comparable results. The two stages are performed in sequence:

1. First stage – V-shape indentation

To perform the V-shape indentation stage, the unit-cell was mounted in the laboratory tool and properly fixed. The tool is then installed in the hydraulic press and the V-punch screwed to the upper plate of the press. The V-shape indentation stage is represented in the corresponding row of Table 4.6, with the V-punch schematic representation and the joining stage apparatus. A perfect alignment between the edge of the V-punch and the tenon's symmetry plan must be ensured to allow splitting the free-length precisely in two equal flanges by opening a groove through the polymer core layer. Angle θ is set to be 45º and the displacement d_1 is dependent on the free-length l_t. It was intended that the groove (say edge of the V-punch) end at $0.5\ mm$ length from the mortise panel.

2. Second stage – Upset compression

Following the V-shape indentation stage is the upset compression stage with a flat punch, represented in the last rows of Table 4.6. To have comparable results to the joints produced with the single-stage joining process, the punch displacement d_2 was set to obtain a head joint length, l_h, of approximately $0.5\ mm$.

Table 4.6 - Two-stage joining test: experimental procedure

Test	**Composite sandwich panel**	**Specimen**	**Free-length dimensions**		
Two-stage joining test	Litecor®	Unit-cell	$t\ (mm)$	$w_t\ (mm)$	$l_{t_i}\ (mm)$
			2	10	$1, 1.5, 2, 2.5, 3.5$
Stage	**Test scheme**	**Punch**	**Test apparatus**		
1. V-shape indentation $d_1 = l_{t_i} - 0.5\ (mm)$	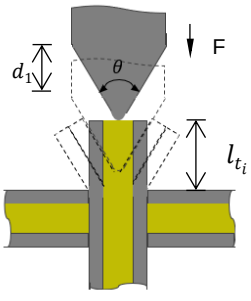	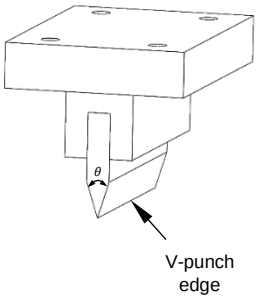	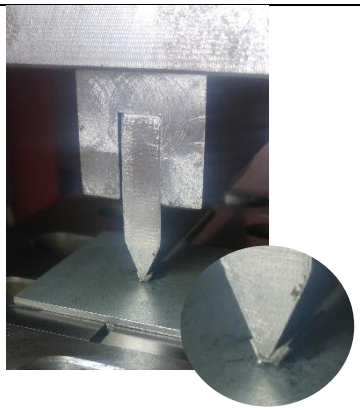		

2. Upset compression $d_2 = l_{V_{ident_i}} - 0.5\ (mm)$	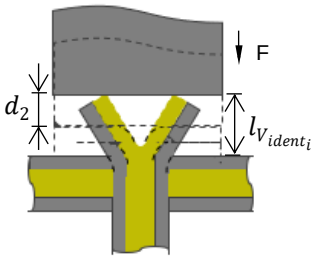	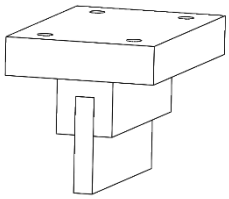	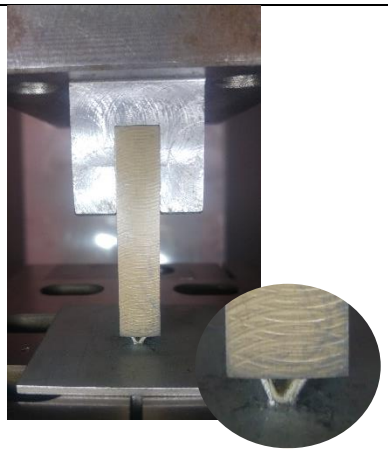

4.3.4.3. Three-stage joining test

The experimental work plan for this process and the experimental apparatus of each stage is presented in the following Table 4.7. Five tests were performed, the joining tests started with the higher stable length of the single-stage joining process and, from this length forward, four joining tests were performed increasing $0.5\ mm$ in the second test and $1\ mm$ in the following tests. The three stages are performed in sequence:

1. **First stage – Polymer Cutting**

   In this very first stage the polymer layer is removed using a saw blade as represented in polymer cutting stage line of Table 4.7. The volume of polymer layer cut corresponds to a saw blade displacement of $d_1 = l_t - 0.5\ mm$. At the end of this step, the free-length is made of two steel flanges, separated by a small polymer layer of $0.5\ mm$ length.

2. **Second stage – Nosing**

   For the Nosing stage, the unit-cell was mounted in the laboratory tool and properly fixed. The tool is then installed in the hydraulic press in such a way that the cavity of the U-concave punch must be aligned with the tenon's symmetry plan. Both, the U-concave punch schematic representation and the joining stage apparatus are represented in Nosing stage line of Table 4.7. The punch action allows to inner bend the tips of the steel flanges. The flat part of the U cavity has $0.5\ mm$ and the curved part has a radius of $1\ mm$. The punch displacement d_2 is dependent on the free-length l_{t_i}.

3. **Third stage – Upset compression**

   The third and final stage is the upset compression stage, in which the main plastic deformation occurs, and the head joint gets its final shape. The displacement of the flat punch d_3 is defined to form a final head joint length l_h in a range between $0.5 - 1\ mm$. The details are shown in the final lines of Table 4.7.

Table 4.7 - Two-stage joining test: experimental procedure

Test	**Composite sandwich panel**	**Specimen**	**Free-length initial dimensions**		
Three-stage joining test	Litecor®	Unit-cell	$t\ (mm)$	$w_t\ (mm)$	$l_{t_i}\ (mm)$
			2	10	$2, 2.5, 3, 4, 5$
Stage	**Test scheme**	**Punch**	**Test apparatus**		
1. Polymer Cutting $d_1 = l_{t_i} - 0.5\ (mm)$	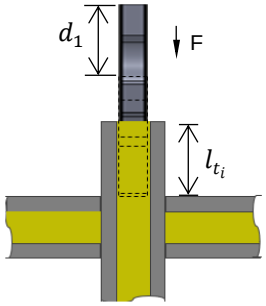	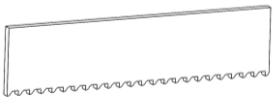			
2. Nosing $d_2 = 1\ mm$	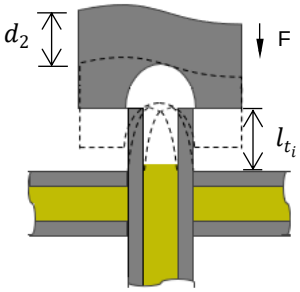	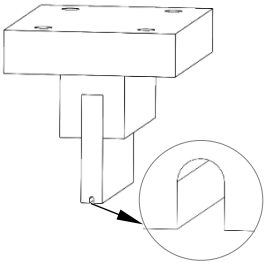	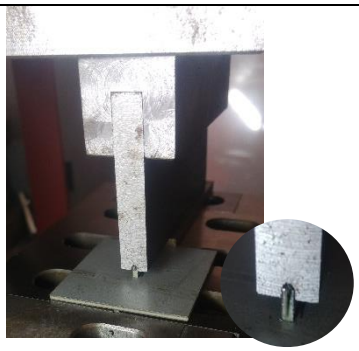		
3. Upset compression $d_3 = l_{nosing_i} - 0.75\ (mm)$	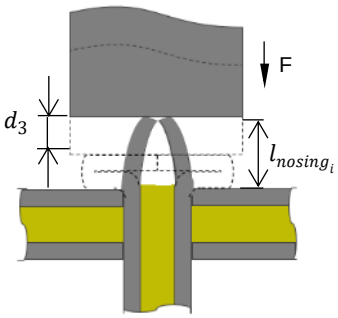	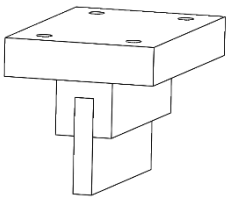			

4.3.5. Destructive tests

To finalize the experimental procedure, the performance of the joints produced by each joining by forming method is assessed by means of destructive tests aimed at determining the force to detach the two sandwich panels. The second and final process parameter considered is the maximum force to detach the two Litecor® panels.

The destructive tests performed are tensile pull-out tests, in which the joint is subjected to uniaxial tensile load.

- **Laboratory tool**

The laboratory tool used is represented in Figure 4.9 and it was designed to prevent deformation by bending during the application of tensile forces.

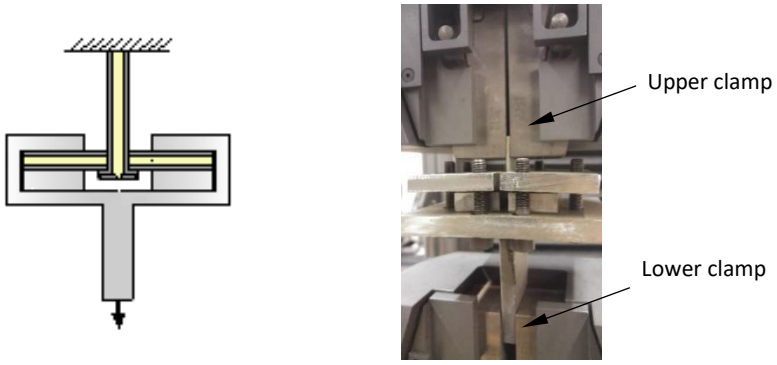

Figure 4.9 - Destructive test: Laboratory tool (schematic representation) and test apparatus

- **Procedure**

The test is performed in the universal testing machine at room temperature with a velocity of 1 mm/min. The work plan defined for the destructive tests are resumed in Table 4.8. All the fifteen joints were tested to evaluate their performance. The unit-cell joints were mounted and properly fixed in the laboratory tool. The tool was then installed in the universal testing machine as represented in Figure 4.9, the upper clamp of the machine holds the Litecor® panel directly and the lower clamp holds the tool in the opposite direction.

As in the joining tests, the load exerted on the joint by the clamps of the universal testing machine is extrapolated as a function of its displacement, and it is possible to observe how the evolution of the force exerted occurs and its maximum value. It is also intended to understand the failure mode of the joint, tracking the critical section of the joint under this loading type.

Table 4.8 - Experimental work plan for the Destructive test

Test	Material		Specimen					
Destructive test	Litecor®		Unit-cell joints					
l_t	1	1.5	2	2.5	3	3.5	4	5
1. Single-stage	✓	✓	✓	✓	-	✓	-	-
2. Two-stage	✓	✓	✓	✓	-	✓	-	-
3. Three-stage	-	-	✓	✓	✓	-	✓	✓

5. Results and Discussion

This chapter presents the results obtained from the experimental work and from the numerical simulation performed, as well as a discussion of them.

It is divided in four subchapters. The **first subchapter** concerns the instability test results. **The second subchapte**r presents the joints produced experimentally and approaches a comparison between numerical and experimental results obtained through the different phases of the joining processes. The **third subchapter** presents and discusses the results of the destructive tests performed. Finally, the **fourth subchapter** presents a real structure joined by the three-stage joining by forming process developed.

5.1. Instability test

The first task in the development of the joining processes was the determination of the critical length l_{cr} that gives rise to plastic instability in the form of buckling out of the sheet plane by upset compression of the tenon. The occurrence of buckling compromises the success of the process as it causes asymmetric deformation of the head joint. Thus, it is useful to know when it happens and how it could be avoided.

Among the three joining processes, the single-stage is the one that can fail by buckling so, for this reason, the results of this test were directly used in its development. However, they also helped decide on the experimental work plan of the two and three-stage joining processes.

Different test specimens with various l_0 were employed (refer to the l_0 values of Table 4.3). The photographic details of the specimens tested are shown in Table 5.1. Only the specimens with significant deformation are represented. Figure 5.1 shows the corresponding experimental and finite element predicted evolutions of the force with displacement for each plastic behaviour of the instability tenons.

It is possible to identify two different plastic behaviours:

- For tenon length values below the critical length $l_0 < l_{cr}$, failure by out-of-plane buckling does not occur. The results show that the range of the stable behaviour is $l_0 \in [1.5, 2, 2.5, 3, 3.5, 4]$. This interval leads to symmetric modes of deformation (refer to the column “Stable” of Table 5.1). The curve evolution for the stable behaviour of $l_0 = 3.5$, is shown in Figure 5.1a). It is characterized by an initial steep rise in the force until the punch travels $0.2\,mm$. This initial compression promotes the delamination of the sandwich panel (steel sheets unsticking the polymer core layer) and the force increases now at a lower rate until the steel sheets start to curve. The steel sheets deform in a curved shape at a constant force, the force stabilizes at around $7.5\ \mathrm{kN}$. For high displacement of the punch, the steel panels start to overlap, offering more resistance to be plastic deformed, that justifies the force increasement in the final part of the test.
- Instability tenons greater or equal to the critical length, $l_0 \geq l_{cr}$, behave differently due to the occurrence of out-of-plane buckling. The unstable behaviour happens for $l_0 \geq 4.5$, in this interval the resulting deformation is non-symmetrical (refer to the column “Unstable” of Table 5.1). Figure 5.1 b) shows the experimental and numerical predicted evolution of the force with displacement for a tenon

with initial length of $l_0 = 4.5\,mm$. A first steep increase of the force with displacement is presented when the flat punch touches the tenon. The force continues to increase at a lower rate, up to a maximum force of around $7.5\ \mathrm{kN}$. When buckling occurs and the curved configuration is reached, the specimen with $l_0 \geq l_{cr}$ experience a secondary loading path in which the compression force decreases. It is required less force when the tenon buckles into the new curved configuration. No delamination is observed, the tenon deforms as a single material column.

As seen, the agreement between the experimental and numerical evolution of the force with displacement is good for both behaviours.

Table 5.1 - Photographic details of the instability specimens tested

$l_0\ (\mathrm{mm})$			
Stable			Unstable
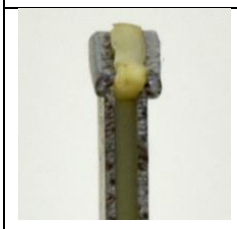		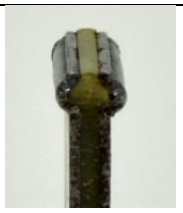	
$l_{0_1} = 3$	$l_{0_2} = 3.5$	$l_{0_3} = 4$	$l_{cr} = 4.5$

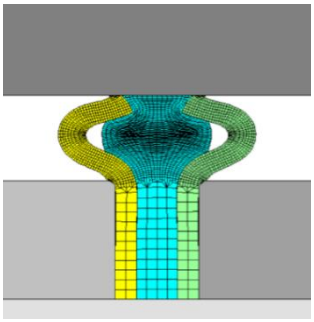

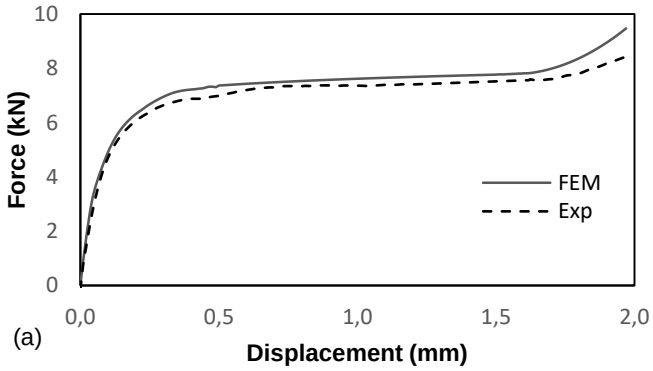

(a)

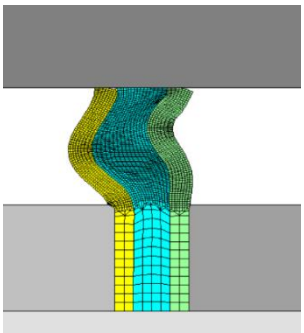

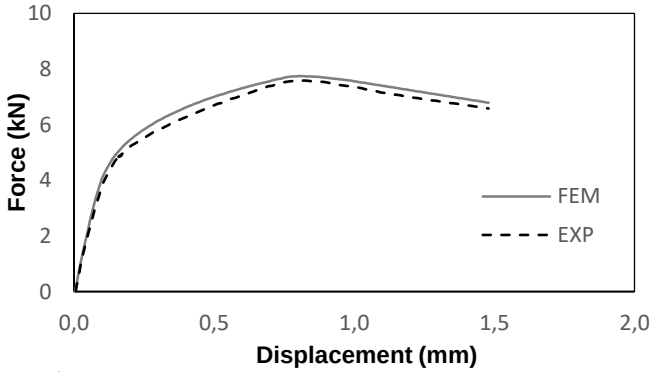

(b)

Figure 5.1 - Experimental and finite element predicted evolution of the force with displacement for the instability test of two specimens with initial length of: a) $\mathrm{l_0 = 3.5\ mm}$ and b) $\mathrm{l_0 = 4.5\ mm}$.

The success of the single-stage joining process is dependent on l_{cr}.To effectively transpose the results of the instability test to the single-stage joining test it is noteworthy to mention the geometrical conversion between both, shown in Figure 5.2.

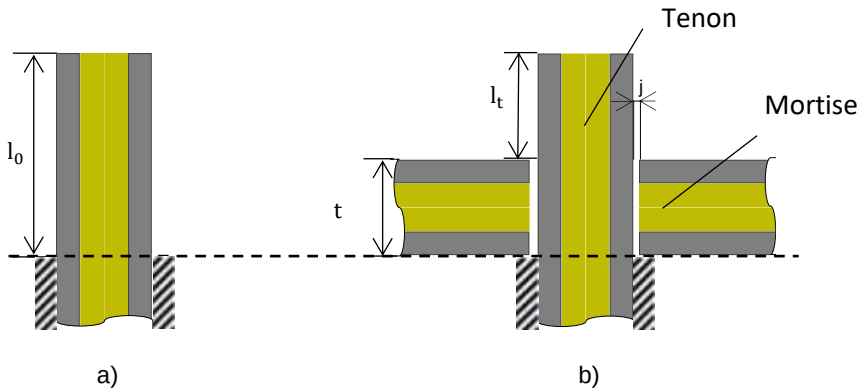

Figure 5.2 - Dimensional comparison between a) Instability tenon and b) Unit-cell

In the instability test, the length of the specimen that will suffer buckling failure is the one that is not cantilevered, dimension l_0 of Figure 5.2 a). The corresponding l_0 dimension in the joining test is the sum $\mathrm{t} + l_t$, as represented in Figure 5.2 b), where t corresponds to the thickness of the Litecor® panels ($2\ mm$) and l_t is the free-length of the tenon, responsible for the interlocking which creates the joint. So, the lengths can be matched, as followed

$$l_{0_i} = \mathrm{t} + l_{t_i} \qquad (6)$$

Table 5.2 - Instability test specimen vs Joining test specimen – geometrical conversion

$l_{0_i} = \mathrm{t} + l_{t_i}$	l_{0_i}	t	l_{t_i}
$i = 1$	~~1.5~~	2	~~-0.5~~
$i = 2$	~~2~~	2	~~0~~
$i = 3$	~~2.5~~	2	~~0.5~~
$i = 4$	**3**	2	**1**
$i = 5$	**3.5**	2	**1.5**
$i = 6$	**4**	2	**2**
$i = 7$	$\boldsymbol{l_{0_{cr}}}$**=4.5**	2	$\boldsymbol{l_{t_{cr}} = 2.5}$

Based on the instability test results and knowing the geometrical conversion defined by equation (6) and represented in Table 5.2, it can be concluded that:

- The first three instability tests performed, $l_0 \in [1.5, 2, 2.5]$, are not valid because the corresponding free-length of the tenon l_t in the single-stage joining process is not enough for the formation of the mechanical interlocking.

- The single-stage joining process may be stable for $l_0 \in [3, 3.5, 4]$ which is equivalent to $l_t \in [1, 1.5, 2]$.
- The single-stage joining process may be unstable for $l_t \geq 2.5$ because $l_{0_{cr}} = 4.5\ mm$.

5.2. Joining by forming processes

This subchapter shows the joints obtained by every joining process, as well as the results achieved experimentally and numerically for each phase of the joining processes.

- **Obtained joints**

By performing the whole experimental process, it was possible to successfully obtain three types of joints, they are shown in Figure 5.3. Under this thesis' study, a joining by forming process is considered successful to join steel sandwich panels, if it creates a firm and robust joint achieved through a symmetrical mechanical lock – the head joint - formed under controllable and stable plastic deformation conditions capable to withstand reasonable tensile loads.

All the mechanical joints obtained allowed a full interlocking of the Litecor® panels with thickness t = $2\ mm$, perpendicular to one another, in a T-shape joint configuration, eliminating the clearance between the tenon and mortise panels and creating firm joints.

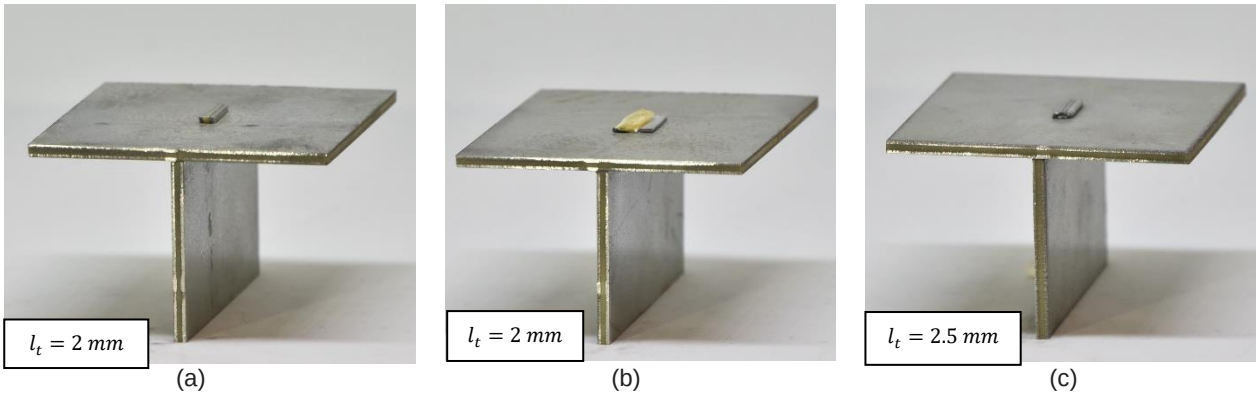

(a) (b) (c)

Figure 5.3 - Experimental results obtained from each joining process: (a) Single-stage joining process; (b) Two-stage joining process; (c) Three-stage joining process;

5.2.1. Single-stage joining process

In the single-stage joining process, the plastic deformation process occurs in only one stage, by a uniaxial open-die forging – flat upset compression. The joining process begins when the flat punch touches the tenon and ends after the punch as completed its downward movement d.

Five different free-lengths l_t of the tenon were tested (refer to Table 4.5), and the overall results show good agreement with those obtained in the previous section of tenon's instability test.

The predictions based on the instability test results were verified. In fact, when the free-length of the tenon in the unit-cell is less or equal to the critical length $l_t < 2.5\ mm$, there are no signs of out-of-plane buckling so symmetrical head joints are formed. On the other hand, for free-length values greater than

the critical length $l_t \geq l_{cr} = 2.5\ mm$, the joint is considered unsuccessful due to asymmetrical formation of the head joint.

Now, taking a detailed discussion on the single-stage process results, it can be identified two different modes of deformation by means of self-explanatory schematic symbols, Table 5.3.

Table 5.3 - Schematic representation of the deformation modes observed in the single-stage joining by forming process for the entire set of tests.

$l_t\ (mm)$				
1	1.5	2	2.5	3.5
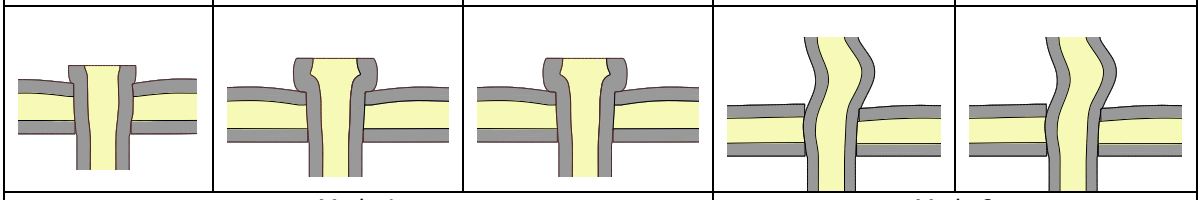				
Mode 1			Mode 2	

In mode 1, during the uniaxial forging, the tenon is compressed and its side faces are forced to deform in the thickness direction along of $t + l_t$ (Figure 5.2b). They undergo a phenomenon of curvature referred to as a barrelling effect originated in the frictional forces that develop at the punch-tenon interface. In the single-stage joining process, the barrelling effect is the phenomenon originating the joint interlocking. It is intended that the barrelling effect develop symmetrically and be as sharp as possible to obtain a larger resistant area, greater mechanical interlocking and, therefore, a more robust joint.

The plastic deformation of mode 1 takes place in two phases:

- In phase one, the tenon is compressed and hence the length of the tenon $t + l_t$ reduces and the thickness t increases to occupy the volume corresponding to the gap j, being w_t x t x j (mm^3). This phase ends when the gap is filled making the tenon length t to be constrained by the mortise.
- Phase two is focused on the plastic deformation of the free-length of the tenon, l_t. As the punches continue to move downward and the tenon length t, corresponding to the gap j, being now constrained by the mortise, this will result in the deformation of the free-length, l_t. In this moment the joint interlocking is created as the free-length's thickness is progressively increasing until it creates the final head joint. Note that the deformation of tenon length surrounded by the mortise continues to enlarge in such a way that the steel layers of the tenon are penetrating the polymer layer of the mortise as it can be seen in the zoomed section of Figure 5.4b.

In mode 1, as the free-length l_t increases, the size of the flat shaped head becomes larger. The lowest free-length tested, l_{t_1}, gave rise to symmetric flow of material however, the surface expansion was considered too small resulting in an insufficient interlocking between the two Litecor® panels. For this reason, joints produced under deformation mode 1 with $l_t \leq 1\ mm$ are classified as inappropriate due to insufficient interlocking.

The minimum free-length $l_{t_{min}}$ to perform the single-stage joining process is 1.5 mm, $l_{t_{min}} = 1.5\ mm$.

The deformation mode 1, for $l_t \in [1.5, 2]$, is typical of sound (appropriate) joints having thickness t_h of the flat-shaped head larger than 1.5 times the original thickness t of the cross section, like what is commonly found for the head and tail diameters of cylindrical rivets.

The deformation mode 2 is typical of slender tenons (say, $l_t > 2\,mm$) and is triggered by plastic instability (buckling) and asymmetric outward material flow. The joints produced under deformation mode 2 are classified as inappropriate.

The process window for the single-stage joining process is then:

$$l_t \in [l_{min}, l_{cr}] = [1.5, 2]$$

Figures 5.4 a) and b) show the photographic details and the corresponding finite element predicted geometries of the cross section of two joints produced under deformation modes 1 and 2. The flow of material obtained in the numerical simulations is similar to the one observed experimentally.

Figure 5.4 c) and d) shows the experimental and finite element evolutions of the force with displacement for the two modes of deformation of the single-stage mortise-and-tenon joint applied to Litecor® sandwich panels. The overall agreement between experimental and numerical results is very good with only small discrepancies. They may be justified due to the existence of a slight deformation towards the width and the numerical simulation was performed under plane strain plastic deformation conditions.

In case of mode 1, there is a monotonic growth of the force with displacement as a result of the progressive compression of the flat-shaped head of the tenon against the lower sandwich composite panel containing the mortise. The small peak increase force after $d = 0.5\,mm$ takes into account the transition between the two phases of mode 1. To initiate phase 2, it is required more force to deform the free-length of the tenon and to create the mechanical interlocking of the joint.

In case of mode 2, the evolution of the force with displacement deviates from that of mode 1 due to compensation of the increase in force due to strain hardening and surface expansion with the reduction in force caused by asymmetric material flow due to plastic instability (buckling) of the tenon.

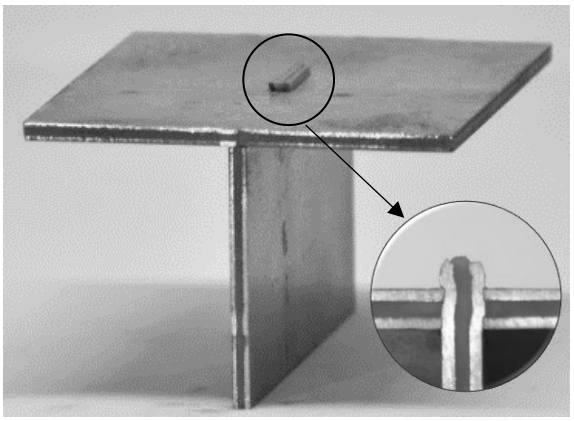

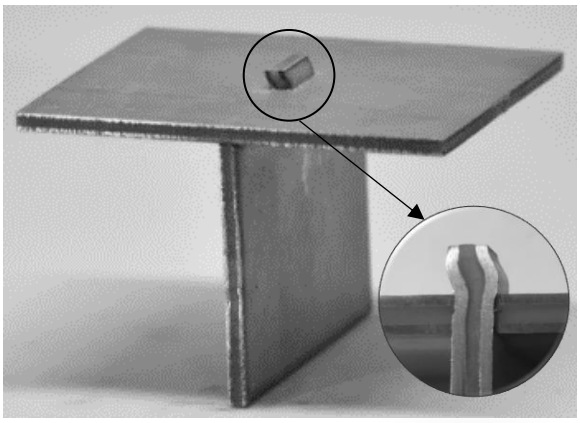

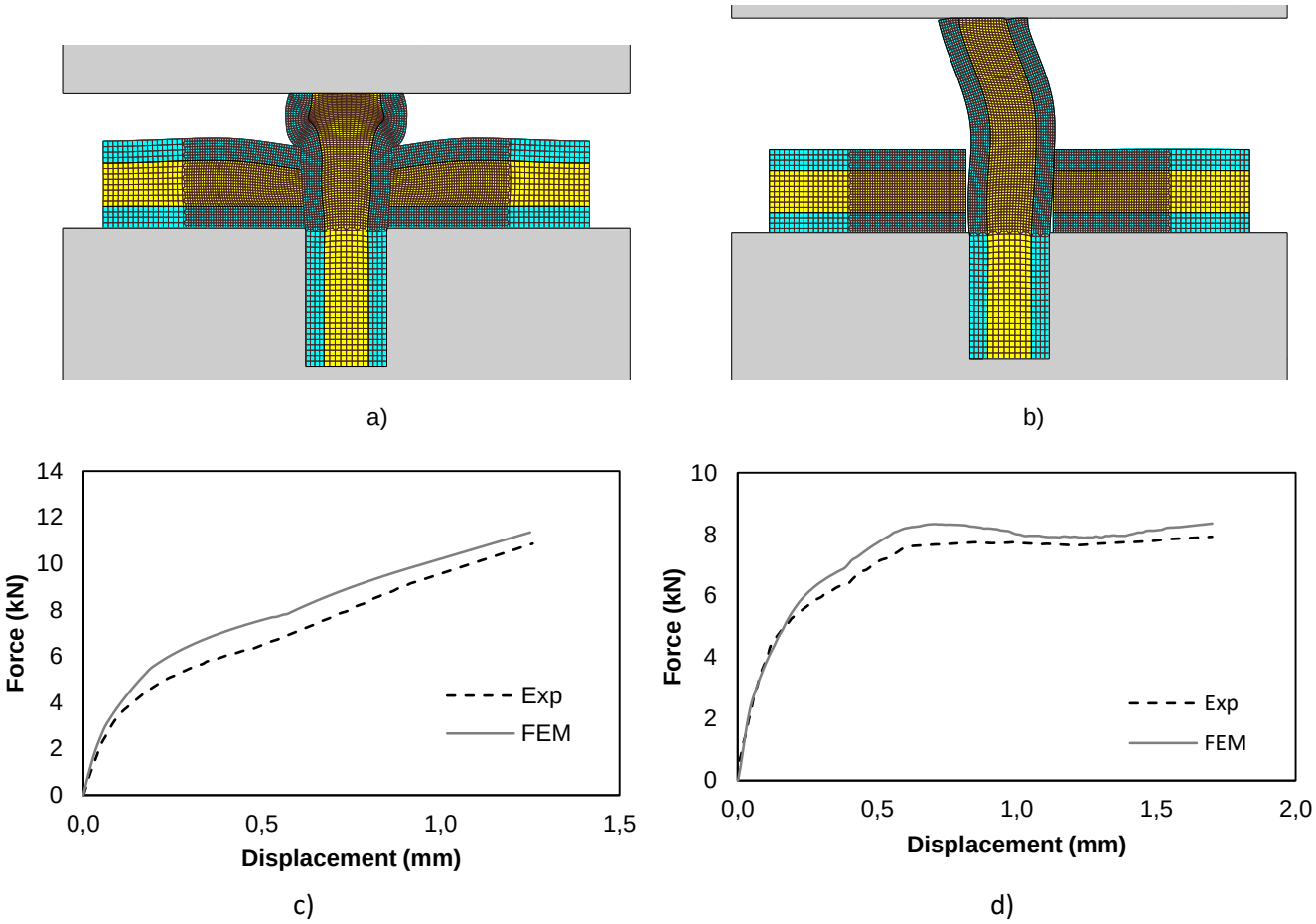

Figure 5.4 - Assembling two Litecor® sandwich composite panels perpendicular to one another by means of single-stage joining by forming: photograph and finite element predicted cross section of a joint produced under a) deformation mode 1 ($l_t = 2\,mm$), b) deformation mode 2 ($l_t = 3\,mm$); Evolution of the upset compression force with displacement for typical joints produced under c) deformation mode 1 ($l_t = 2$ mm) d) deformation mode 2 ($l_t = 3.5$ mm).

5.2.2. Two-stage joining process

Figure 5.5 shows an example for a tenon with $t = 2.5$ mm, which would give rise to an inappropriate joint if single-stage joining by forming was used (Table 5.3). Similar examples could be provided for the entire range of process parameters listed in Table 4.7.

In general terms, the two-stage joining by forming process splits the thickness of the tenon into two parts, bends each part along the V-shape surface of the indentation punch and upsets each part against the lower sandwich composite panel containing the mortise.

The correlation between the experimental behaviour and finite element predicted cross sections, Figure 5.5 a) and b), and between the measured and computed force vs. displacement evolutions, Figure 5.5 c) and d), are good for both stages of the process.

The first stage, V-shape indentation, is characterized by low forces. The punch's action causes the tenon to split by the opening of a groove in the polymer layer (ductile material) as a consequence the steel flanges are bended in a 45º angle imposed by the punch included angle, θ. As the V-punch moves downwards, the groove is opening continuously making the polymer layer to flow in

the direction of the width of the tenon, w_t. A negligible elastic recovery is presented after the indentation process, however in no way it compromises the following stage.

The material behaviour in the numerical simulation was restricted to plane strain deformation (2D). In the V-shape indentation stage, the flow of the polymer layer does not follow is not two-dimensional it flows perpendicular to the V-punch movement. However, for the deformation of the steel sheets it is verified 2-D deformation conditions and because its strength is much higher than the polymer it will dictate the evolution of the force-displacement graphs.

The differences observed between the experimental and numerical curves of the V-shape indentation stage may be justified by the friction value used for the interface of the V-punch-polymer layer. The one used in the simulations was a lower one, 0.1, to facilitate the simulation model and avoid sticking of the elements in the model. The real friction coefficient must be higher because the FEM curve is under the experimental curve.

In the second stage, flat upset compression stage, when the punch touches the flanges there is a sudden increase in force, followed by a reduction in force. The force decreases during the pure bending of the $0.5\ \mathrm{mm}$ steel flanges. As soon as the steel flanges touch the mortise panel, the force of the punch increase to press them and ensure a full mechanical interlocking.

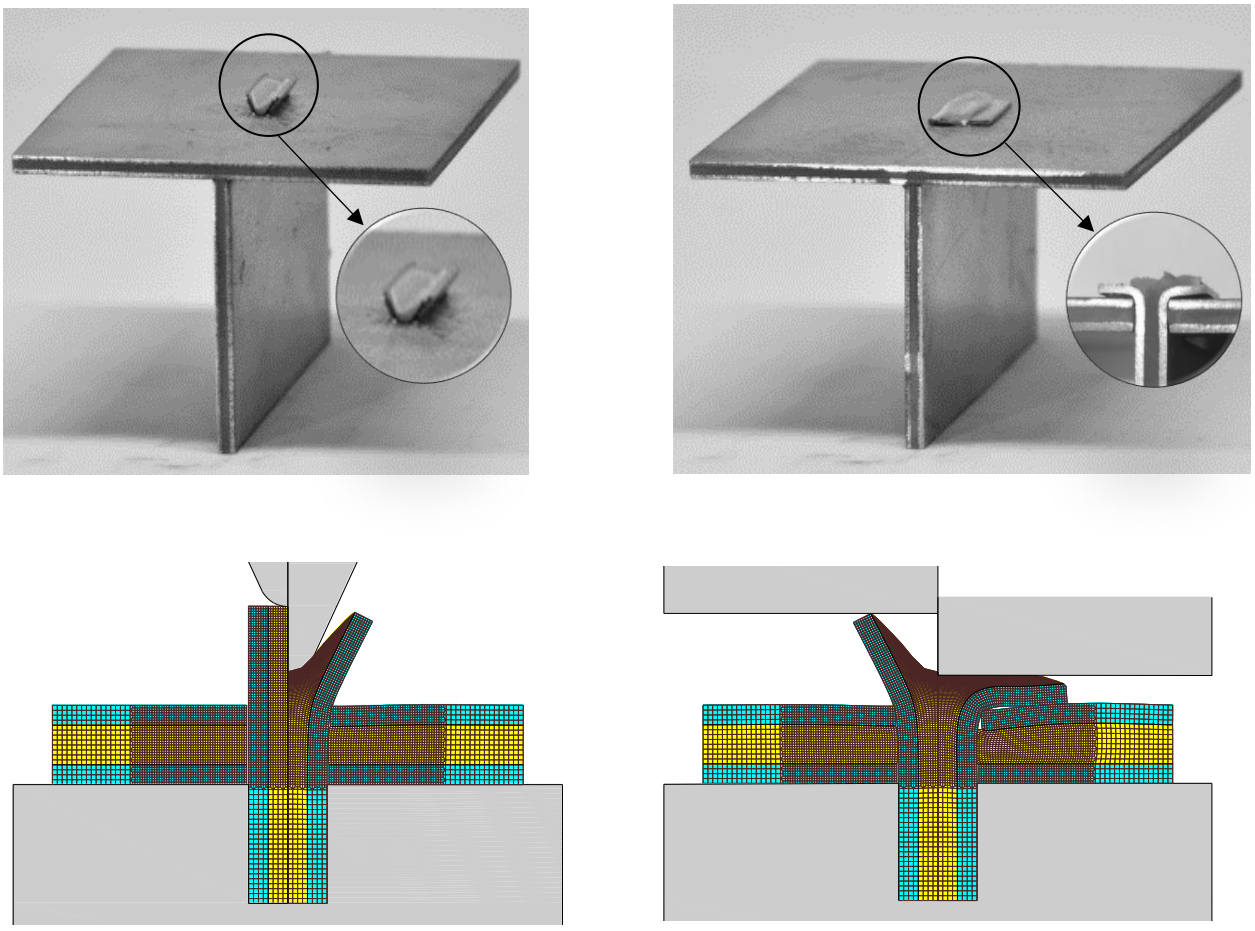

a) b)

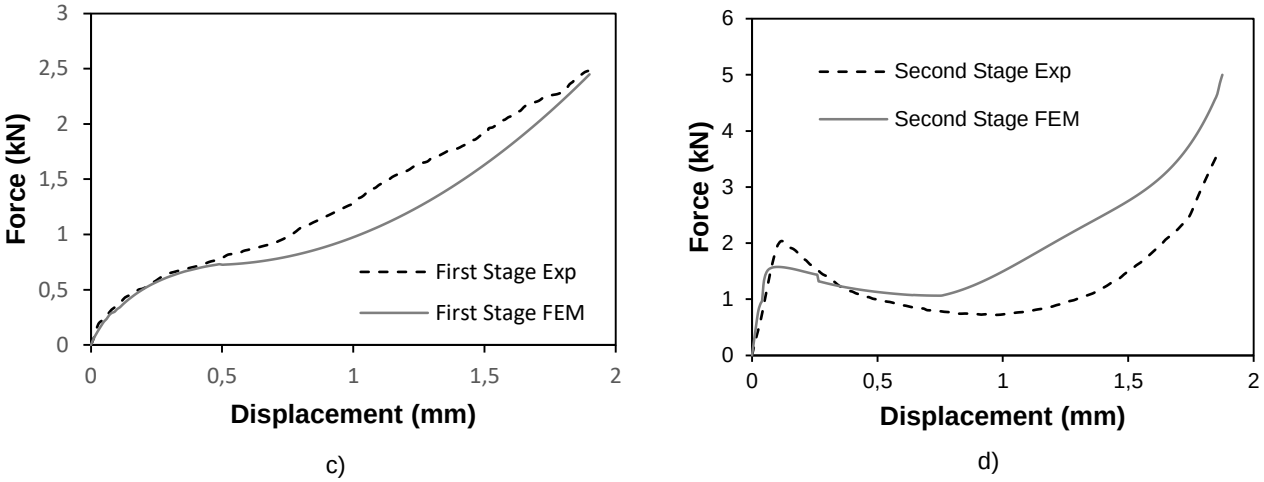

Figure 5.5 - Assembling two Litecor® sandwich composite panels perpendicular to one another by means of the new proposed two-stage joining by forming: Photograph and finite element predicted cross section of a joint at a) the beginning and end of the first stage ($l_t = 2$ mm), b) the beginning and end of the second stage ($l_t = 2$ mm); Evolution of the force with displacement for c) V-shape indentation stage; d) Upset compression stage

5.2.3. Three-stage joining process

The three-stage joining by forming process is the solution to circumvent the above-mentioned problems of plastic instability of the single-stage joining by forming process applied to sandwich composite panels and to simultaneously increase the flat-shaped head and strength of the mechanically locked joints.

As shown in Figure 5.6 a) and b) the process is carried out in three stages comprising cutting out the polymer core of the tenon placed above the surface of the mortise followed by nosing and flat punch upsetting of the outer thin metal sheets of the tenon.

In the first stage, Polymer cutting stage, the polymer layer is removed leaving the tenon with the two steel flanges isolated as desired for the consequent plastic deformation operations. No significant records were taken in this stage. It must be ensured that the saw blade does not damage the steel flanges. Working with such small steel sheet thicknesses, $t_s = 0.5\,mm$, even a small scratch may influence the further plastic deformation operations.

The last two stages are utilized to form a compression bead that will increase the pull-out forces due to metal reinforcement of the flat shaped head of the joint. The overall agreement between the experimental and numerical predicted cross-sectional geometries is very good.

In the Nosing stage, the fixed punch displacement $d_2 = 1\,mm$ proved to be enough to keep the edge tips of the steel flanges in contact and avoid an excessive elastic strain recovery, see the zoomed section of Figure 5.6 a). Regarding the evolution of the force with displacement, Figure 5.6 c), show a monotonic growth of the force as the steel flanges travel along the curved section of the U-concave punch. It is a process characterized by low forces.

In the final stage, the steel flanges undergo flat upset compression. In this stage the major plastic deformation occurs, and the compression bead is formed. The Force-displacement curve, Figure 5.6 d), is much more complex than the one of the Nosing stage. Even so, the overall agreement between the

numerical and experimental is very good. A three-region trend is observed in the upset compression stage. The first region is characterized by an initial steep increase of the force, when the flat punch touches the bended steel flanges. In the second region the average force is constant, and it corresponds to the constant deformation on the steel sheets into the final shape of the head joint (refer to the zoomed area of photograph in Figure 5.6 b)). The third region presents a steep increase of the force as the flat-shaped head of the tenon is pressed against the lower sandwich composite panel containing the mortise. In this region a slight discrepancy between the two curves is observed. This can be explained because for high displacements of the punch the approximation of plane strain deformation is not so realistic.
The joining process force is below 15 kN allowing it to be easily performed with low cost equipment.
As shown also in the finite element simulation results included in Figure 5.6, the new proposed process can produce large flat-shaped heads from slender tenons because it takes advantage of plastic instability to produce a compression bead instead of being limited by buckling failure, as in case of single-stage joining by forming.

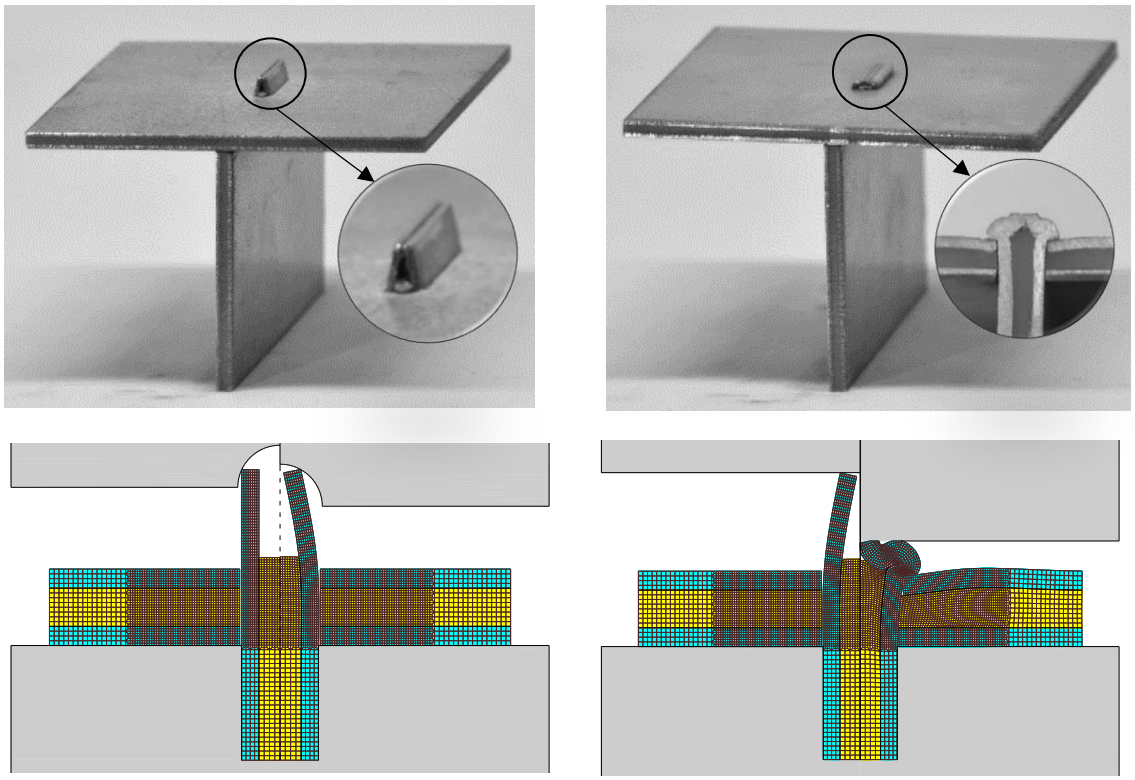

a) b)

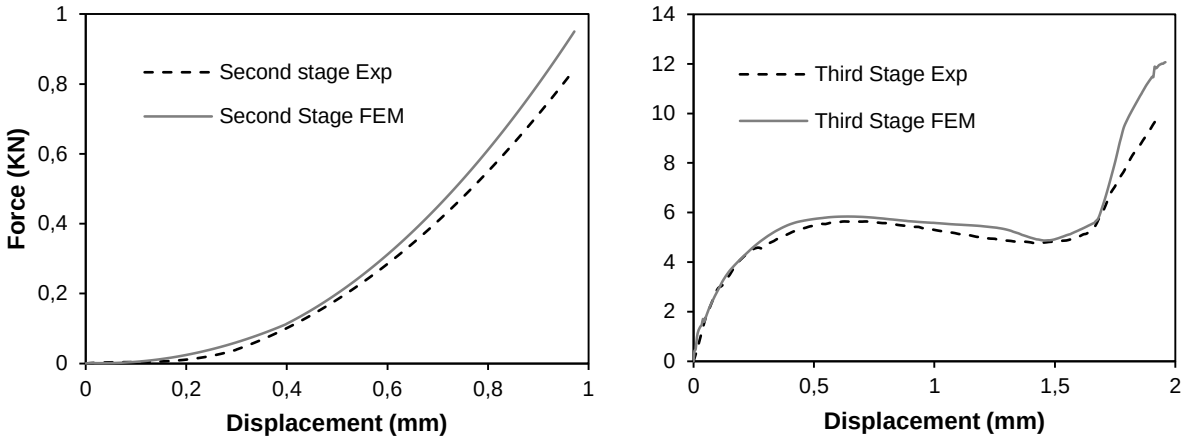

c) d)

Figure 5.6 - Assembling two Litecor® sandwich composite panels perpendicular to one another by means of the new proposed three-stage joining by forming: Photograph and finite element predicted cross section of a joint at a) the beginning and end of the second stage ($l_t = 2.5$ mm), b) the beginning and end of the third stage ($l_t = 2.5$ mm); Evolution of the force with displacement for c) the second stage: Nosing, d) the third stage: Upset compression

5.3. Destructive test

The overall performance of the three joining by forming processes was assess by means of destructive pull-out tests aimed at determining the maximum force that the joints are capable to withstand before failure. The tests were carried out for the entire set of unit-cells produced from each joining process.

The results of the test are presented in a graphical format according to the process parameters. The maximum pull-out forces represented in y-axis and the free-length of the tenon in the x-axis, as shown in Figure 5.7 a). The ratio between the maximum strength of the joint and the free-length of the tenon, $F_{máx}/l_t$, should be as large as possible to produce the most robust joints with the lowest amount of material usage.

The results will be discussed process by process, in ascending order of maximum pull-out forces.

The two-stage joining process is the one with the lowest pull-out forces and is the only one that keeps the force constant with increasing the free-length of the tenon. The test show that the pull-out force is independent of the free-length of the tenon with a constant force, $F_{máx} = 2\,\mathrm{kN}$. For this reason, the highest ratio $F_{máx}/l_t$ is happening for $l_t = 1\ mm$. The material usage is minimized, and the strength kept constant.

The single-stage joining process presents a pull-out force increase of around 15% by $0.5\ mm$ increase within the range investigated, $[1.5,2]$. The minimum force corresponds to the joint with the smallest free-length approx $2.82\,\mathrm{kN}$ and the largest corresponds to $3.25\,\mathrm{kN}$. The mechanical interlocking increases with the increase of the free-length and this translates into a greater resistance of the joint. This increasing tendency ends when failure occurs by buckling for $l_t > 2.5\ mm$, [2.5, 3.5]. In these cases, the asymmetric flat-shaped head turns out to be a mixture of the two processes, single-stage (stable behaviour) and two-stage joining processes as schematically represented by the figure of the graph.

This justifies the reduction of maximum joint force to the unstable zone of the single-stage joining process. The highest ratio $F_{máx}/l_t$ corresponds to the joint $l_t = 1.5\ mm$.

When applying the pull-out force to the two-stage and the single-stage joints, they failed by unbending the flat-head back to the longitudinal axis of the tenon, as represented by the dashed lines in the schematic cross section figures of the graph.

The three-stage joining process starts for $l_t = 2\ mm$, with a maximum force of approx. $3.35\ \mathrm{kN}$ close to the force obtained by the corresponding joint of the single-stage joining process. For $l_t = 2.5\ mm$ a significant increase of 35% in the pull- out force is obtained only by increasing l_t in $0.5\ mm$. For $l_t > 2.5\ mm$ the joint resistance remains constant and equal to approximately $F_{máx} = 4.20$ kN. The joints with $l_t \in$ [2.5,5] fail by cracking, instead of pure unbending as in every other joint produced in this work thesis, Figure 5.7 b). The highest ratio $F_{máx}/l_t$ corresponds to $l_t = 2.5\ mm$. The metal reinforcement of the flat-shaped heads caused by metal folding over itself (compression beads) contributes to increase the overall strength of the joint and the pull-out forces that are required to detach the two sheets.

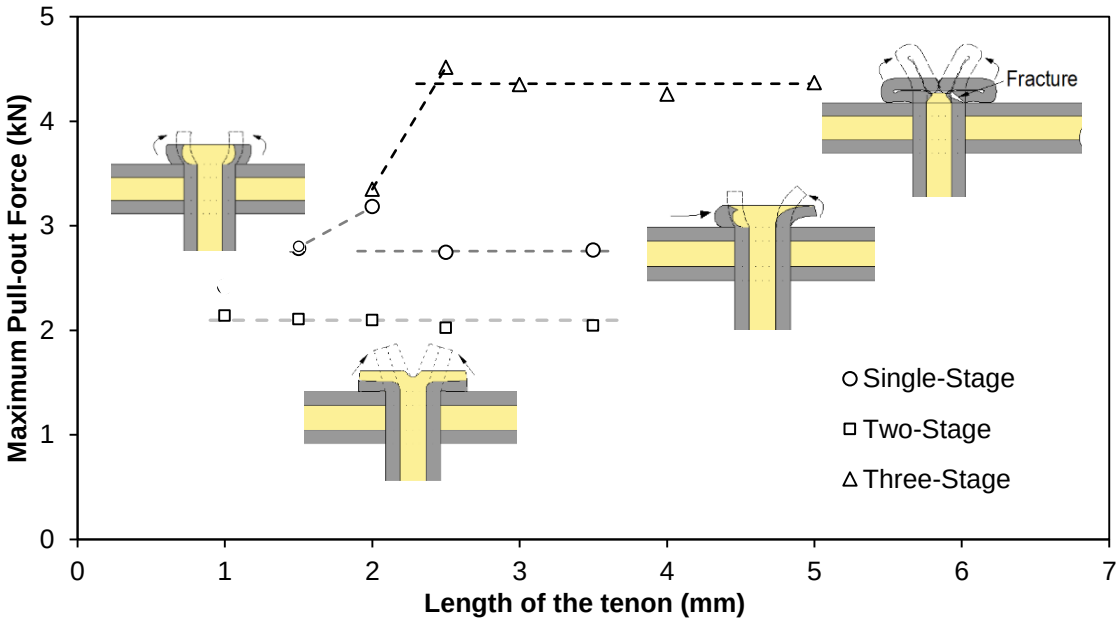

a)

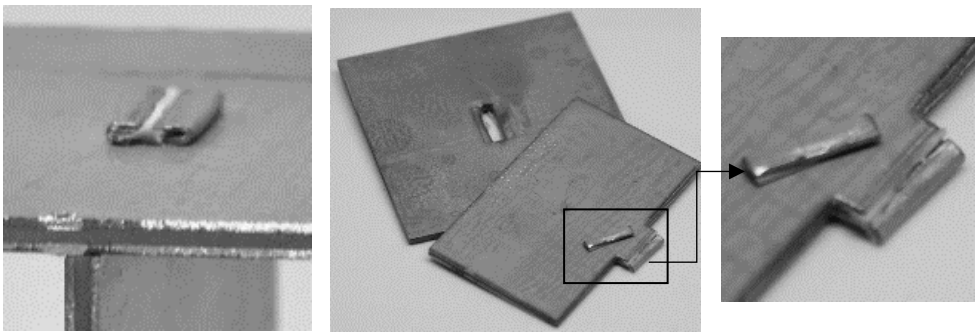

b)

Figure 5.7 - Destructive pull-out tests of the joint produced by the three joining by forming processes: a) Maximum pull-out forces as a function of the length l_t of the tenons; b) Photograph of a joint produced by the three-stage joining by forming process before and after testing;

5.4. Application to the fabrication of lightweight structural panels

This last section presents an example of application of the new three-stage joining by forming process. A lightweight structure made of composite sandwich panels was assembled and joined in a mortise-and-tenon joint configuration. The exploded view of Fig. 5.9 a) shows the several parts, namely the location and orientation of the different tenons and mortises that were utilized to fabricate the panel. The different parts were produced by water jet cutting like the unit-cell elements. The drawings of each part are shown in Appendix B. As seen in Figure 5.8, the tenons and mortises were orientated along two different directions to prevent preferential deformation in a given direction. This structure was joined in the hydraulic press.

Figure 5.8 shows the real panel at two different intermediate stages of assembly and after being produced.

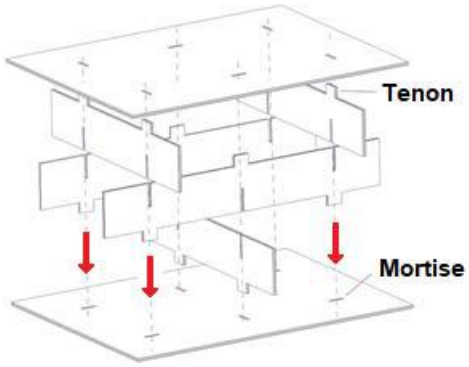

a)

b)

Figure 5.8 - Application of the new joining by forming process to the fabrication of lightweight structural panels: a) Exploded view of the panel and b) photographs showing the real panel at different stages of the assembly.

6. Final Remarks

In this final chapter, it is intended to conclude the investigation performed. This is divided into two sub-chapters. The **first subchapter** presents all the conclusions regarding the case study, presenting considerations about the accomplishments done and a summary of its relevant points. Finally, the **second subchapter** intends to promote some future work with prospects of being carried out in the future towards process maturity.

6.1. Conclusions

This thesis validates the feasibility of the three proposed joining by forming processes to assemble two sandwich composite panels perpendicular to one another, in a T-shape configuration.

It was possible to obtain three types of purely mechanical joints without the need of any type of consumable, thermal influence or extra bonding element. The mortise-and-tenon joints are formed through local plastic deformation of small initial free-lengths of the tenon which means small material usage and low protrusion head joints, $[0.5 - 1mm]$. The mechanical joints allowed a full interlocking of the panels perpendicular to one another, eliminating the clearance between the tenon and mortise panels and creating robust joints capable to withstand reasonable tensile loads.

Regarding the numerical and experimental results for each stage of the joining processes, there was a good correlation, both concerning the flow of material and final head joint visual aspect as well as the graphical evolution of the load exerted by the punch as a function of the displacement.

Although the results showed that single-stage joining by forming, which was originally developed for metal sheets, can be successfully applied to sandwich composite panels, its workability window is limited. Slender tenons with $l_t > 2$ mm will buckle and give rise to unacceptable asymmetric flat-shaped heads of the joints. This limits the maximum pull-out forces that these joints can safely withstand and justify the reason why the development of two alternative joining processes.

The two-stage joining process is an effective process easy to implement however it has the lowest joint strength which for some applications may be acceptable for others may not.

Thus, among the three joining solutions, the three-stage joining process reveals to be the most promising solution in terms of process window workability and robustness (maximum pull-out strength). This innovative three-stage solution comprises, cutting out the polymer core of the tenon placed above the surface of the mortise followed by nosing and flat punch upsetting of the outer thin metal sheets of the tenon, allows producing mechanically locked joints that can withstand pull-out forces up to 4.2 kN. Failure of these joints is by cracking of the flat-shaped head instead of unbending. The three-stage joining by forming process produces mechanically locked joints with larger and stiffer flat-shaped heads than those fabricated by conventional single-stage mortise-and-tenon solutions. Despite being reinforced with metallic compression beads, these joints still need less than 15 kN to be produced. This makes the new proposed process an effective, inexpensive, solution for joining sandwich composites with affordable simple equipment and to make the use of these materials more affordable and widespread in industry.

Compared with the current available joining processes applied to composite sandwich panels, described in subchapter two of the state of the art, some advantages can be seen with respect to some of the joining processes:

- Being a cold mechanical joining process so there is no chance of polymer deterioration by heat input, keeping the physical integrity of the composite sandwich panel (great advantage compared with welding joining processes);
- Weight savings, no extra components nor added materials are used resulting in lower joint weight compared to mechanical fastening processes (screws or rivets and SPR);
- No surface preparation is required, the joint is produced in the as received condition, which results in improvements on the joining cycle time when compared to adhesive bonding;
- Low production costs because it is a joining process which requires low forces and low-cost equipment;

6.2. Future works

Future works must be focused in several aspects:

- Studying the influence of the sandwich panel thickness t to be joined as well as the variation of the width mortise-tenon, w_t. This would require an extensive experimental study in which the various geometrical limits mentioned above would be understood in greater detail.
- Studying this joining technology in a multi-material design concept, which means, investigation of joints between dissimilar material pairings such as: Litecor®-Al, Litecor®-PC , Litecor®-AHSS.
- Perform a wide variety of joint testing namely fatigue and fluency tests to be compared with conventional processes.

References

[1] D. Kodjak, "Policies to Reduce Fuel Consumption, Air Pollution and Carbon Emissions from Vehicles in G20 Nations," The International Council on Clean Transportation, 2015.

[2] European comission, “Reducing CO2 emissions from passenger cars” [Online]. Available: https://ec.europa.eu/clima/policies/transport/vehicles/cars_en [Accessed in 15th April 2018].

[3] MIT, “On the road in 2035” [Online]. Available: http://web.mit.edu/sloan-auto-lab/research/beforeh2/otr2035/On%20the%20Road%20in%202035_MIT_July%202008.pdf [Accessed in 5th May 2018].

[4] Statistica, “Proportion of vehicle parts in total passenger car weight” [Online] Available: https://www.statista.com/statistics/275304/proportion-of-vehicle-parts-in-total-passenger-car-weight/ [Accessed in 9th May 2018].

[5] Don Rosato, "NPE 2015 end-use regulatory impact review: Automotive lightweighting,". [Online]. Available: http://exclusive.multibriefs.com/content/npe-2015-end-use-regulatory-impact-review-automotive-lightweighting/engineering [Accessed 27th June 2018].

[6] Sigarra, “Caracterização mecânica do material compósito LITECOR para um processo de conformação plástica” [Online]. Available: https://sigarra.up.pt/feup/pt/pub_geral.pub_view?pi_pub_base_id=201548. [Accessed in 1st June 2018]

[7] Bolay C.: Beitrag zur Umformung von ebenen und versteiften Schichtverbundwerkstoffen. Dissertation. Universität Stuttgart, Stuttgart, Deutschland, 2014.

[8] Buhl J.: Umformverhalten und Grenzen von Schichtverbundwerkstoffen. Dissertation. Universität Siegen, Siegen, Deutschland, 2014.

[9] Nutzmann M.: Umformung von Mehrschichtverbundblechen für Leichtbauteile im Fahrzeugbau. Dissertation. RWTH Aachen, Aachen, Deutschland, 2008.

[10] Sokolova O.: Study of metal/polymer/metal hybrid sandwich composites for the automotive industry. Dissertation. TU Clausthal, Clausthal-Zellerfeld, Deutschland, 2012.

[11] Automotive manufacturing solutions, “Joining the dots” [Online]. Available: https://automotivemanufacturingsolutions.com/technology/joined-up-thinking-2 [Accessed in 13th May 2018]

[12] ResearchGate, “Composite Materials” [Online] Available: https://www.researchgate.net/publication/318760692_Chapter_16_Composite_Materials [Accessed in 10th June 2018]

[13] Vinson JR. Sandwich structures: Past, present and future. 7th International Conference on Sandwich Structures, Aalborg, Denmark 2005, 3-12.

[14] Davies, J.M. Ed.: Lightweight sandwich construction. Blackwell Science, Oxford, Malden, MA, 2001.

[15] S. Mousa and G.-Y. Kim, "A Direct Adhesion Metal-Polymer-Metal Sandwich Composite by Warm Roll Bonding," Journal of Materials Processing Technology, vol. 239, p. 133–139, 2017.

[16] S. Mousa and G.-Y. Kim, "Experimental Study on Warm Roll Bonding of Metal/Polymer/Metal Multilayer Composites," Journal of Materials Processing Technology, vol. 222, pp. 84-90, 2015.

[17] Hayashi H. and Nakagawa T.: Recent trends in sheet metals and their formability in manufacturing automotive panels. Journal of Materials Processing Technology, 1994 (46), P. 455–487.

[18] Kim J.-K. and Yu T.-X.: Forming and failure behaviour of coated, laminated and sandwiched sheet metals. a review. Journal of Materials Processing Technology, 1997 (63), P. 33–42.

[19] Alucobond® USA, "Alucobond PE tech data" [Online], Available: https://www.alucobondusa.com/products.html [Accessed in 18th August 2018]

[20] Bondal®, "bondal®" [Online], Available: http://www.thyssenkrupp-materials-processing-europe.pl/en/products/coated-sheet/organic-coated-sheet/bondal.html [Accessed in 18th August 2018]

[21] Hylite®, "Hylite®" [Online], Available:https://www.display.3acomposites.com/hylite.html [Accessed in 18th August 2018]

[22] Litecor®, "Litecor®" [Online], Available: https://www.thyssenkrupp.com/en/company/innovation/cross-industry-innovation/litecor.html [Accessed in 18th August 2018]

[23] Steelite®, "Steelite, a steel prolypropylene laminate" [Online], Available: https://www.tandfonline.com/doi/pdf/10.1179/174329306X122802?needAccess=true [Accessed in 18th August 2018]

[24] Usilight®, "USILIGHT: A Cost-Effective Solution to Lighten Cars" [Online], Available:https://www.sae.org/publications/technical-papers/content/2006-01-1216/ [Accessed in 18th August 2018]

[25] ThyssenKrupp, "Solutions for automotive efficiency" [Online], Available: https://www.thyssenkrupp-components-technology.com/media/publikationen/thyssenkrupp_incar_plus_executive_summary_english.pdf [Accessed in 25th March 2018]

[26] ThyssenKrupp, "Higher-strength IF steels HX" [Online]. Available: https://www.thyssenkrupp-steel.com/en/download [Accessed in 27th March 2018]

[27] Thyssenkrupp, "Litecor®, The new way to build lighter cars" [Online]. Available: https://www.thyssenkrupp.com/media/publikationen/thyssenkrupp_techforum/2013/techforum_1_13_en.pdf [Accessed in 30th March 2018]

[28] ThyssenKrupp, "Litecor" [Online] Available: https://www.thyssenkrupp.com/en/company/innovation/cross-industry-innovation/litecor.html [Accessed in 6th April 2018]

[29] ThyssenKrupp, "the sandwich effect" [Online] Available: http://www.thyssenkrupp.com.cn/upload/accessory/201412/20141229157529036 49.PDF [Accessed in 24th April]

[30] tc, "Thermally Induced Stresses Due to Coefficient of Thermal Expansion Mismatch in Hybrid Metallic/Composite Structures", [Online]. Available: http://www.tc.faa.gov/its/worldpac/techrpt/tctn17-41.pdf [Accessed in 29th July 2018]

[31] Europe, T.S. (2013). Litecor®, Technical Information Sheet. Duisburg – Germany: ThyssenKrupp Steel Europe AG.

[32] Richard Anthony Davis. "Delamination of Sandwich composites" [Online], Available: https://digitalcommons.calpoly.edu/cgi/viewcontent.cgi?referer=https://www.google.pt/&httpsredir=1&article=1025&context=aerosp [Accessed in 7th August 2018]

[33] MSE, “Strength of Sandwich structures” [Online], Available: http://www.mse.mtu.edu/~drjohn/my4150/sandwich/sp2.htm [Accessed in 7th August 2018]

[34] Wittrick Wh. A theoretical analysis of the efficiency of sandwich construction under compressive end load. Rep Memo, 2016 (UK Aeronautical Research Council, Farnborough, Hants, UK), 1945

[35] Forging, “glossary forging terms” [Online]. Available: http://site: https://www.forging.org/forging/glossary-forging-terms.html [Accessed in 3rd July 2018]

[36] . ThyssenKrupp, “Application potential of litecor in the body” [Online]. Available: https://www.thyssenkrupp-components-technology.com/media/publikationen/thyssenkrupp_incar_plus_atzextra_english_kl.pdf [Accessed in 2nd April 2018]

[37] Pieronek, D., Böger, T., Röttger, R., (Oct. 2012). Modeling Approach for Steel Sandwich Materials in Automotive Crash Simulations. ThyssenKrupp Steel Europe.

[38] ThyssenKrupp, “Lightweight design in the door outer panel” [Online]. Available: https://www.thyssenkrupp-components technology.com/media/publikationen/thyssenkrupp_incar_plus_atzextra_english_kl.pdf [Accessed in 2nd April 2018]

[39] ThyssenKrupp, “Stiffness-optimized sandwich material Litecor®” [Online]. Available: http://multimedia.3m.com/mws/media/931504O/automotive-fk13-vortrage.pdf [Accessed in 2nd April 2018]

[40] Kinloch, A.J., *Durability of structural Adhesives.* 1983: Applied Science Publishers*.*

[41] Dillard DA. *Advances in structural adhesive bonding*. Cambridge: Woodhead Publishing, 2010.

[42] ResearchGate, “Schematic diagram of adhesive bonding process for aluminium alloys a applying adhesive” [Online]. Available: https://www.researchgate.net/figure/Schematic-diagram-of-adhesive-bonding-process-for-aluminum-alloys-a-Applying-adhesive_fig12_274732062 [Accessed in 17th May 2018]

[43] M.D. Banea and L.F.M. da Silva. (Sep. 2018) Adhesively bonded joints in composite materials: an overview, Proc. IMechE Vol. 223 Part L: J. Materials: Design and Applications

[44] Thyssenkrupp steel, “Dual-phase steel” [Online], Available: https://www.thyssenkrupp-steel.com/en/products/sheet-coated-products/multiphase-steel/dual-phase-steel/ [Accessed in 17th April 2018]

[45] Thyssenkrupp steel, “MBW – manganese boron steel for hot forming” [online], Available: https://www.thyssenkrupp-steel.com/en/products/sheet-coated-products/manganese-boron-steel-for-hot-forming/mbw-manganese-boron-steel-for-hot-forming/ [Accessed in 17th April 2018]

[46] Sagüés Tanco J, Nielsen CV, Chergui A, Zhang W and Bay N. Weld nugget formation in resistance spot welding of new lightweight sandwich material. *International Journal of Advanced Manufacturing Technology* 2015; 80: 1137-1147.

[47] Senkara, J., Zhang, H., and Hu, S. J., (2004). Expulsion Prediction in Resistance Spot Welding. Welding Research, Welding Journal, pp. 123-132.

[48] Ihsan Kadhom Abbas Al Naimi (2015), Weldability of New Material Sandwich Steel for Automotive Applications. Al-Khwarizmi Engineering Journal,Vol. 12, No. 2, P.P. 60- 78 (2016)

[49] ResearchGate, “Weldable vibration damping steel sheet” [Online] Available: https://www.researchgate.net/publication/296577972_Weldable_vibration_damping_steel_sheet [Accessed in 17th April 2018]

[50] Akihiko Nishimoto, Yukichi Watanabe, Yasushi Fujii, Shinji Kabasawa, and Yasunori Matsuda, (1988). Weldable Vibration Damping Steel. NKK Technical Review No. 53.

[51] The welding master, "Laser beam welding" [Online] Available: http://www.theweldingmaster.com/laser-beam-welding/ [Accessed in 23th April 2018]

[52] Salonitis K, Drougkas D, Chryssolouris G (2010) Finite element modeling of penetration laser welding of sandwich materials. Phys. Procedia 5:327–335. DOI 10.1016/j.phpro.2010.08.059

[53] Konstantinos Salonitis & Panagiotis Stavropoulos & Apostolos Fysikopoulos & George Chryssolouris. CO_2 laser butt-welding of steel sandwich sheet composites. Int J Adv. Manuf. Technol (2013) 69:245-256. DOI 10.1007/s00170-013-5025-7

[54] The welding master, "Friction Stir Welding" [Online] Available: http://www.theweldingmaster.com/friction-stir-welding/ [Accessed in 23th April 2018]

[55] Kemplon, "Friction Stir Welding (FSW) & its Affinity for Aluminum" [Online]. Available: http://kemplon.com/wp-content/uploads/2016/03/4-Friction-Stir-Welding-FSW-Process.jpg [Accessed in 23th April 2018]

[56] Patents google, "Friction stir weld bonding of metal-polymer-metal laminates" [Online]. Available: https://patents.google.com/patent/US7628876 [Accessed in 23th April 2018]

[57] R.W. Messler Jr., Joining of Materials and Structures: From Pragmatic Process to Enabling Technology. 2004, Burlington, MA: Elsevier.

[58] C. G. Pickin, K. Young, and I. Tuersley, "Joining of lightweight sandwich sheets to aluminium using self-pierce riveting," Mater. Des., vol. 28, no. 8, pp. 2361–2365, 2007.

[59] Ansatt, "Self-piercing riveting" [Online]. Available: http://www.ansatt.hig.no/henningj/materialteknologi/Lettvektdesign/joining%20methods/joining-mechanical-self%20piercing%20riviting.htm [Accessed in 25th April 2018]

[60] Jonkers, B. November 2006. Simulation of the robot roller hemming process [Online]. Available: http://essay.utwente.nl/58315/1/graduate_bjonkers.pdf [Accessed in 27th May 2018]

[61] Bob Vila "How to: Make a Mortise and Tenon Joint" [Online]. Available: https://www.bobvila.com/articles/2138-how-to-make-a-mortise-and-tenon-joint/ [Accessed in 20th Augusto 2018].

[62] Verdigrismetals "Mortise and tenon joints" [Online], Available: http://www.verdigrismetals.co.uk/mortise%20and%20tenon%20joints.htm [Accessed in 21th September 2018]

[63] I. M. F. Bragança, C. M. A. Silva, L. M. Alves e P. A. F. Martins, "Joining sheets perpendicular to one other by sheet-bulk metal forming," The International Journal of Advanced Manufacturing Technology, vol. 89.1, pp. 77-86, 2017.

[64] I. M. F. Bragança, C. M. A. Silva, L. M. Alves e P. A. F. Martins, "Lightweight joining of polymer and polymer-metal sheets by sheet-bulk forming," Journal of Cleaner Production, vol. 145, pp. 98-104.

[65] Merklein M, Tekkaya AE, Brosius A, Opel S, Koch J (2011) Overview on Sheet- Bulk Metal Forming Processes. Proceedings of the 10th International Conference on Technology of Plasticity, 1109–1114.

[66] Merklein M, Tekkaya AE, Brosius A, Opel S, Kwiatkowski L, Plugge B, Schunck S (2011) Machines and tools for sheet-bulk metal forming. Key Eng Mater 473:91–98

[67] Mori K, Bay N, Fratini L, Micari F, Tekkaya AE (2013) Joining by plastic deformation. CIRP Ann Manuf Technol 62:673–694

[68] Nielsen CV, Zhang W, Alves LM, Bay N, Martins PAF (2013) Modelling of thermo-electro-mechanical manufacturing processes with applications in metal forming and resistance welding. Springer-Verlag, London, UK

[69] P. Martins, “FINITE ELEMENT FLOW FORMULATION Lecture 1 - Fundamentals and Computer Implementation,” Technical University of Denmark and the University of Aalborg, 2011.

[70] Flowwaterjet, “Mach-3-Brochure [Online]. Available: https://www.flowwaterjet.com/FlowWaterjet/media/Flow/8_Footer/Resources/Downloads/Brochures/Mach%203/Mach-3-Brochure_EN.pdf [Accessed in 5th September 2018]

[71] IST, “Área científica de Tecnologia Mecânica e Gestão Industrial - Laboratório,” [Online]. Available: https://fenix.tecnico.ulisboa.pt/downloadFile/3779572577294/MT_lab.pdf. [Accessed in 1st September 2018].

[72] IST, “Área científica de Tecnologia Mecânica e Gestão Industrial - Laboratório,” [Online]. Available: https://fenix.tecnico.ulisboa.pt/downloadFile/3779572577293/MPT_lab.pdf [Accessed in 1st September 2018].

[73] Alves, L.M., Nielsen, C.V., Martins, P.A.F., 2011. Revisiting the fundamentals and capabilities of the stack compression test. Exp. Mech. 51, 1565e1572.

Appendix A – Solidworks drawings - Mortise and Tenon elements of the Unit cell

- 3D Unit cell

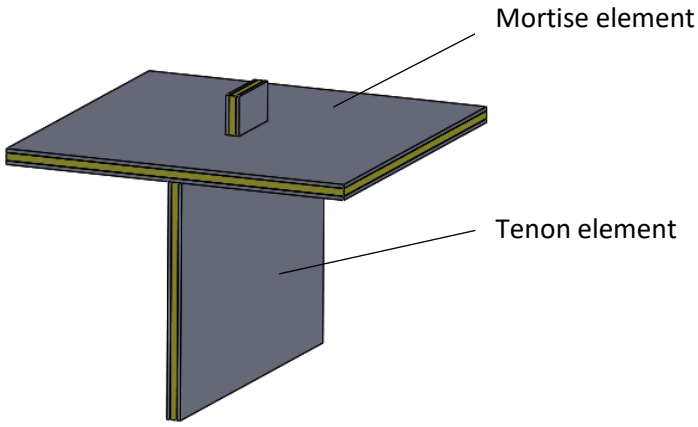

- Solidworks drawings for water-jet cutting

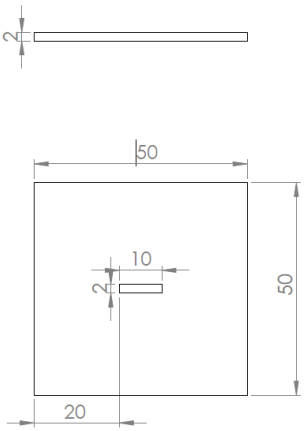

Mortise element

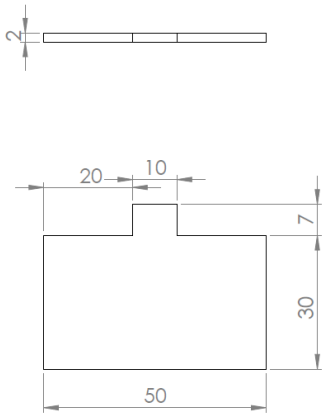

Tenon element

Appendix B –Solidworks drawings – Composite sandwich panel structure joined by the three-stage joining by forming process

- 3D Litecor® structure

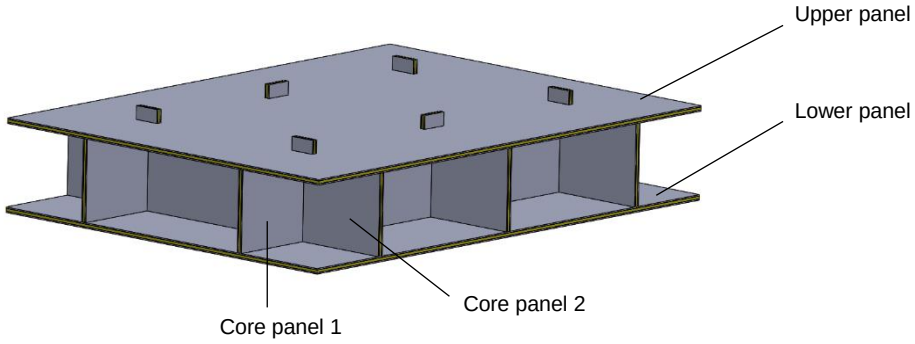

- Solidworks drawings for water-jet cutting

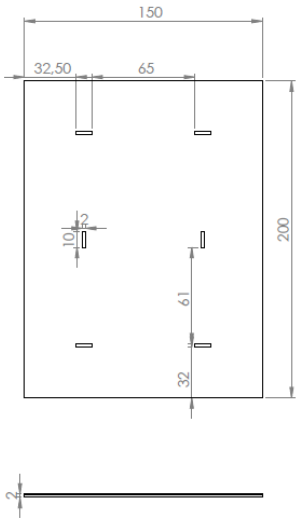

Upper panel

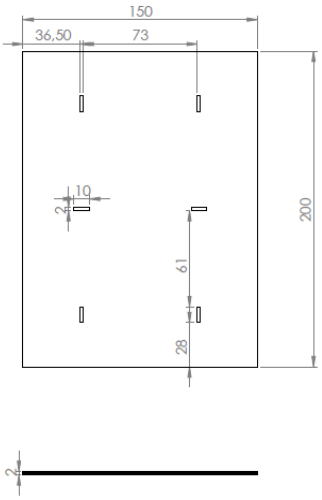

Lower panel

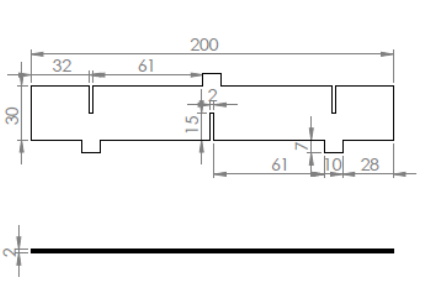

Core panel 1

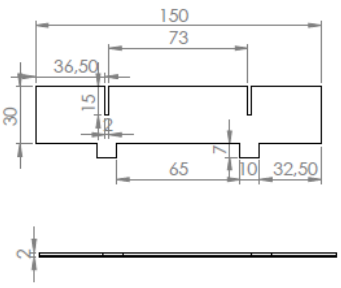

Core panel 2